NASA/USRA

HIGH ALTITUDE RESEARCH AIRCRAFT

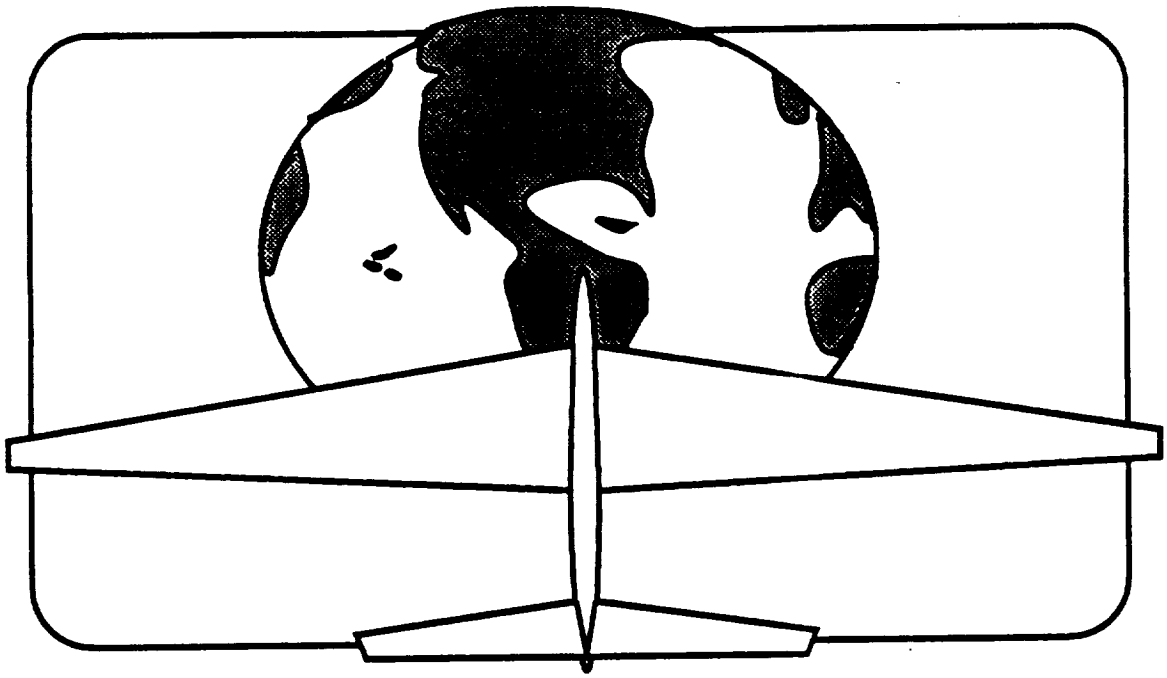

VOLUME 1

SUBMITTED - 1 JULY 1990

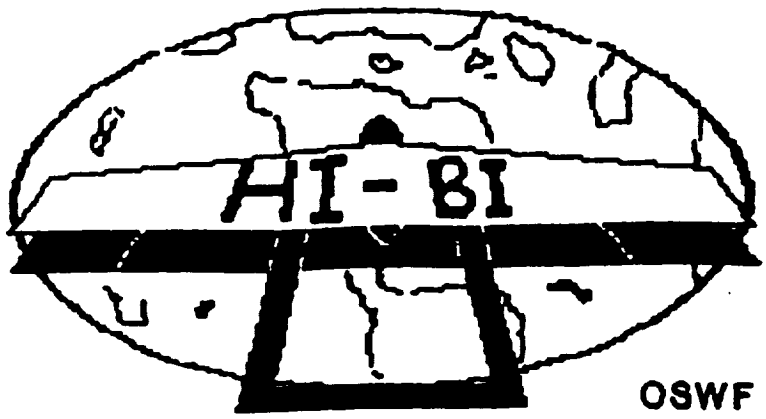

OSWF INDUSTRIES

CALIFORNIA STATE
POLYTECHNIC UNIVERSITY
POMONA

NASA/USRA
HIGH ALTITUDE RECONNAISSANCE AIRCRAFT

GROUP MEMBERS

MICHAEL RICHARDSON

JUAN GUDINO

KENNY CHEN

TAI LUONG

DAVE WILKERSON

ANOOSH KEYVANI

MICHAEL MEDICI - PROJECT ENGINEER

TABLE OF CONTENTS

APPENDIX B

COST BREAKDOWN

APPENDIX C

MAINTAINABILITY & AVAILABILITY ANALYSIS

LIST OF SYMBOLS

Symbol	Definition
b	Wing Span
C_d	Total Aircraft Drag Coefficient
c.g.	Center of Gravity Location
c_l	Airfoil Lift Coefficient
C_L	Total Aircraft Lift Coefficient
C_{lmax}	Maximum Airfoil Lift Coefficient
$C_{l\alpha}$	Airfoil Lift Curve Slope
$C_{L\alpha}$	Wing Lift Curve Slope
$C_{mc/4}$	Pitching Moment Coefficient About Airfoil Quarter Chord
C-F	Turbulent Skin Friction Coefficient
C-D-alpha	Variation of Drag Coefficient with Angle of Attack
C-D-u	Variation of Drag Coefficient with Speed
C-L-i-h	Variation of Lift Coefficient with Stabilizer Incidence
C-M-i-H	Variation of Moment Coefficient with Stabilizer Incidence
C-L-alpha	Variation of Lift Coefficient with Angle of Attack
C-L-u	Variation of Lift Coefficient with Speed
C-L-q	Variation of Lift Coefficient with Pitch Rate
C-L-delta-E	Variation of Lift Coefficient with Elevator Deflection
C-L-alpha-dot	Variation of Lift Coefficient with Angle of Attack Rate

Symbol	Definition
C-m-alpha	Variation of Pitching Moment Coefficient with Angle of Attack
C-m-q	Variation of Pitching Moment Coefficient Pitch Rate
C-m-delta-E	Variation of Pitching Moment Coefficient with Elevator Deflection
C-m-alpha-dot	Variation of Pitching Moment Coefficient with Angle of Attack Rate
C-y-beta	Variation of Side Force Coefficient with Sideslip Angle
C-y-p	Variation of Side Force Coefficient with Roll Rate
C-y-r	Variation of Side Force Coefficient with Yaw Rate
C-y-delta-R	Variation of Side Force Coefficient with Rudder Deflection
C-l-beta	Variation of Rolling Moment Coefficient with Sideslip Angle
C-l-p	Variation of Rolling Moment Coefficient with Roll Rate
C-l-r	Variation of Rolling Moment Coefficient with Yaw Rate
C-l-delta-A	Variation of Rolling Moment Coefficient with Aileron Deflection
C-l-delta-R	Variation of Rolling Moment Coefficient with Rudder Deflection
C-n-beta	Variation of Yawing Moment Coefficient with Sideslip Angle
C-n-p	Variation of Yawing Moment Coefficient with Roll Rate
C-n-r	Variation of Yawing Moment Coefficient with Yaw Rate

Symbol	Definition
C-n-delta-A	Variation of Yawing Moment Coefficient with Aileron Deflection
C-n-delta-R	Variation of Yawing Moment Coefficient with Rudder Deflection
CHAR. EQU.	Characteristic Equation
FT	Feet
FT/S	Feet per Second
hp	Horsepower
HORZ.	Horizontal
Ixx	Rolling Moment of Inertia
Iyy	Pitching Moment of Inertia
Izz	Yawing Moment of Inertia
lbs	Pounds
LBS	Pounds
mm	millimeter
M	Mach Number
MAC	Mean Aerodynamic Chord
OEI	One Engine Inoperative
Re	Reynolds Number
RN	Reynolds Number
S	Planform Area
S_G	Ground Roll Distance
S_R	Roll Distance
S_{TR}	Transition Distance
S_{CL}	Climb Distance
S_A	Air Distance
S_{FR}	Free Roll Distance

Symbol	Definition
S_B	Braking Distance
S_{ref}	Reference Area
t/c	Airfoil Thickness to Chord Length Ratio
T	Thrust
VERT.	Vertical
V_{stall}	Stall Velocity
V_{crit}	Critical Velocity
V_{to}	Take-off Velocity
W	Weight

ABSTRACT

At the equator, the ozone layer ranges from approximately 80,000 to 130,000+ feet which is beyond the capabilities of the ER-2, NASA's current high altitude reconnaissance aircraft. The Universities Space Research Association, in cooperation with NASA, is sponsoring an undergraduate program which is geared to designing an aircraft that can study the ozone layer at the equator. This aircraft must be able to cruise at 130,000 feet for six hours at Mach 0.7 while carrying 3,000 lbs. of payload. In addition, the aircraft must have a minimum of a 6,000 mile range. The low Mach number, payload, and long cruising time are all constraints imposed by the air sampling equipment. In consideration of the novel nature of this project, a pilot must be able to take control in the event of unforseen difficulties.

Three aircraft configurations have been determined to be the most suitable for meeting the above requirements, a joined-wing, a bi-plane, and a twin-boom conventional airplane. Although an innovative approach which pushes the limits of existing technology is inherent in the nature of this project, the techniques used have been deemed reasonable within the limits of 1990 technology. The performance of each configuration is analyzed to investigate the feasibility of the project requirements. In the event that a requirement can not be obtained within the given constraints, recommendations for proposal modifications are given.

1.0 INTRODUCTION

In 1974, F. Sherwood Rowland and Mario Molina, chemists at the University of California, theorized that the ozone layer which protects the earth from harmful ultra-violet radiation was being destroyed by chloroflourocarbons. Chloroflourocarbons, or CFC's as they are commonly referred to, are released into the atmosphere from sources like refrigeration systems, styrofoam production facilities, and aerosol cans to name a few.

Rowland and Molina's theory was met with great skepticism by the scientific community when first published. Scientists as well as the general public had difficulty believing that the Earth's survival was being threatened by the use of hair spray and hamburger containers. Now in the 1990's, the evidence accumulated over the last two decades seems to support Rowland and Molina's theory, the Earth's precious ozone layer is disappearing.

Because of the potential consequences of a depleted ozone layer, scientist are desperately trying to investigate this phenomenon. They are however, limited by the present methods of collecting ozone data. Ninety percent of the ozone layer lies 50,000 to 115,000 feet above the earth's surface. NASA's highest flying atmospheric sampling airplane is the ER-2 which has a service ceiling of only 70,000 feet. Clearly the ER-2 would not be able to sample the majority of the ozone layer.

An alternative to the ER-2 is a large weather balloon. Weather balloons are capable of reaching altitudes of 115,000 feet and beyond but they lack the directional control required for sampling specific target areas. Still another alternative would be rockets carrying sampling equipment. Rockets, however, fly at Mach numbers that are not compatible with current atmospheric sampling equipment.

Clearly there is a need for an aircraft that can effectively sample this region of the Earth's atmosphere. It is for this reason that NASA and the USRA developed a request for proposal for a high altitude reconnaissance aircraft. The request for proposal for the aircraft is listed in appendix A. The performance requirements stated in the RFP are listed below;

1.1 REQUIREMENTS AND CONSTRAINTS

1. The cruise altitude will be 130,000 feet.
2. The required payload will be 3,000 pounds.
3. The design cruise Mach number will be M=0.7
4. The cruise (data sampling) time will be six hours.
5. There is a minimum of one crew member responsible for piloting the aircraft.
6. A 6,000 mile range is required.

1.2 MISSION PROFILE

The mission profile is shown in figure 1.1. The RFP states that the total mission range is 6,000 feet. The RFP also specifies that the sampling time, or time at cruise altitude should be 6 hours. The range and time calculations do not coincide with each other. Six hours at altitude at 0.7 Mach number correspond to a range of 3035 miles. If the HI-BI was limited to six hours at cruise, then the climb and descent legs would have to cover nearly 3,000 miles to make up the rest of the 6,000 mile required range. Trade-off studies using energy methods were performed to determine the most efficient combination of climb, cruise, descent legs. It was calculated that the optimum time at cruise should be 10.9 hours with a 5519.6 cruise range. The total mission range meets the range requirement specified in the RFP but exceeds the sampling time requirement by 4.9 hours.

2.0 INITIAL DESIGN

2.1 DESIGN CRITERIA

After reviewing the aircraft requirements listed in section 1; certain assumptions about the aircraft were made. One of these assumptions was that the aircraft would be required to have a low wing loading due to the low dynamic pressure at the 130,000 ft cruise altitude. Another assumption made was that the aircraft would be propeller

driven due to the subsonic cruise requirement. Further, the airplane would be required to have low drag due to the difficulty in producing thrust at high altitudes.

2.2 CONFIGURATIONS

Possible configurations were considered for the aircraft. These aircraft are listed in Figures 1.2 through 1.6. The flying wing in Figure 1.2 was considered for its lack of horizontal tail and therefore its overall aerodynamic efficiency. The aircraft would also provide a large uninterrupted area to mount ozone sampling devices (large leading edge). Further review of the flying wing showed that the aircraft would require an expensive stability augmentation system due to its inherent instability. The aircraft would also require a long heavy landing gear to accommodate the propellers and was therefore rejected.

Two conventional monoplanes are shown in Figure, 1.3a and 1.3b. A monoplane would be inherently more stable than a flying wing and is a proven design configuration. The preliminary weight and size estimations showed that the airplane would have a wingspan of 600 feet due to the aircraft's low wing loading. The conventional monoplanes were ruled out due to the large required wingspan.

A canard was added to the monoplane as shown in Figure 1.4. The three surface configuration was considered for its

improved aerodynamic efficiency over the standard monoplane. The configuration was ruled out however, because of the interference effects of the canard on the main wing and the destablizing effects of the canard configuration compared to convectional area.

The joined wing configuration shown in Figure 1.5 was seriously considered for the aircraft. The aircraft would be more aerodynamically efficient than the conventional monoplane but without the inherent instability found in the flying wing configuration. The major drawback in incorporating a joined wing would be that the production of a joined wing aircraft would require the development of new technologies as there are no large joined wing aircraft in existence.

FIGURE 1.2
FLYING WING

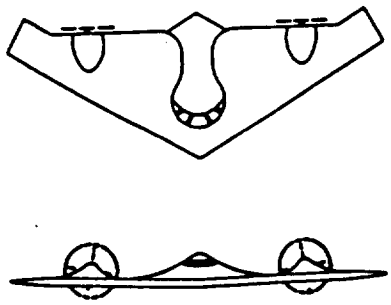

ADVANTAGES

- HIGH AERODYNAMIC EFFICIENCY DUE TO THE LACK OF A HORIZONTAL TAIL
- LARGE FRONTAL AREA AVAILABLE FOR INSTALLING SAMPLING DEVICES

DISADVANTAGES

- INHERENT INSTABILITY
- LANDING GEAR/PROP CLEARANCE
- POOR TAKEOFF ROTATION

FIGURE 1.3a
MONOPLANE - CONVENTIONAL FUSELAGE

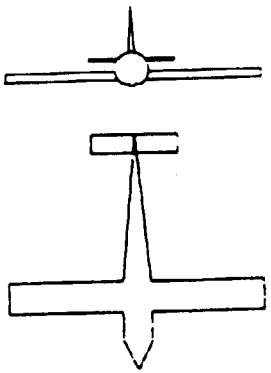

ADVANTAGES

- STABILITY
- EASILY MODELED ON COMPUTERS
- COULD BE BUILT WITH CURRENT TECHNOLOGY

DISADVANTAGES

- WOULD REQUIRED AN EXTREMELY LARGE WINGSPAN
- LARGE BENDING MOMENT ON THE WING ROOT
- LANDING GEAR/PROPELLER CLEARANCE

FIGURE 1.3b
MONOPLANE - TWIN BOOM FUSELAGE

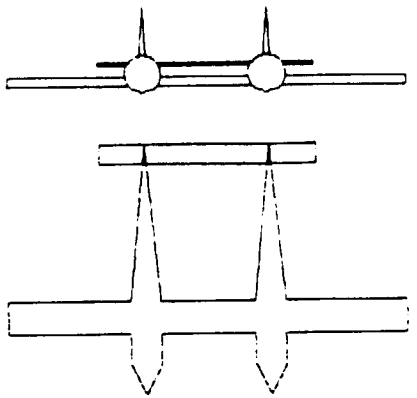

ADVANTAGES

- STABILITY
- EASILY MODELED ON COMPUTERS
- COULD BE BUILT WITH CURRENT TECHNOLOGY

DISADVANTAGES

- WOULD REQUIRED AN EXTREMELY LARGE WINGSPAN
- LANDING GEAR/PROPELLER CLEARANCE

FIGURE 1.4
CANARD

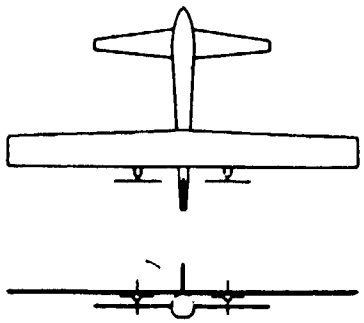

ADVANTAGES

- AERODYNAMIC EFFICIENCY
- REDUCED TRIM DRAG

DISADVANTAGES

- INHERENTLY UNSTABLE
- INTERFERENCE EFFECTS
  ROOT
- LANDING GEAR/PROPELLER CLEARANCE

FIGURE 1.5
JOINED WING

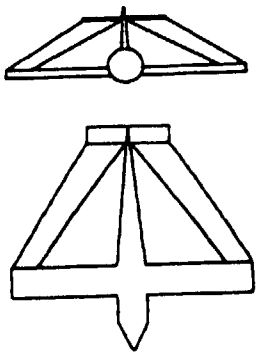

ADVANTAGES

- AERODYNAMIC EFFICIENCY
- STRUCTURAL STRENGH

DISADVANTAGES

- INABILITY TO MODEL ON COMPUTERS
- LARGE JOINED WING AIRCRAFT HAVE NOT BEEN PROVEN TO BE PRACTICAL
- MAY REQUIRE THE DEVELOPMENT OF FUTURE TECHNOLOGY

FIGURE 1.6
TWIN-BOOM BIPLANE

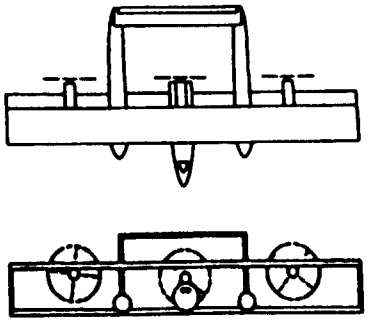

ADVANTAGES

- MAXIMIZES PLANFORM AREA/MINIMIZES SPAN
- STRUCTURAL STRENGH
- LANDING GEAR/PROPELLER CLEARANCE
- LARGE FRONTAL AREA AVAILABLE FOR INSTALLING SAMPLING DEVICES

DISADVANTAGES

- INTERFERENCE EFFECTS FROM THE WING STRUTS

The final configuration was the biplane shown in Figure 1.6. The biplane configurations maximizes planform area while minimizing span. The biplane would thus have a shorter wingspan then that of the monoplane while generating the same lift. The configuration is inherently stable and would have a more conventional structure than the joined wing. The engines on the biplane could be mounted on the top wing, thus solving the problem of propeller clearance and landing gear size. The biplane configuration was thus adopted for the high altitude aircraft.

High Altitude BIplane

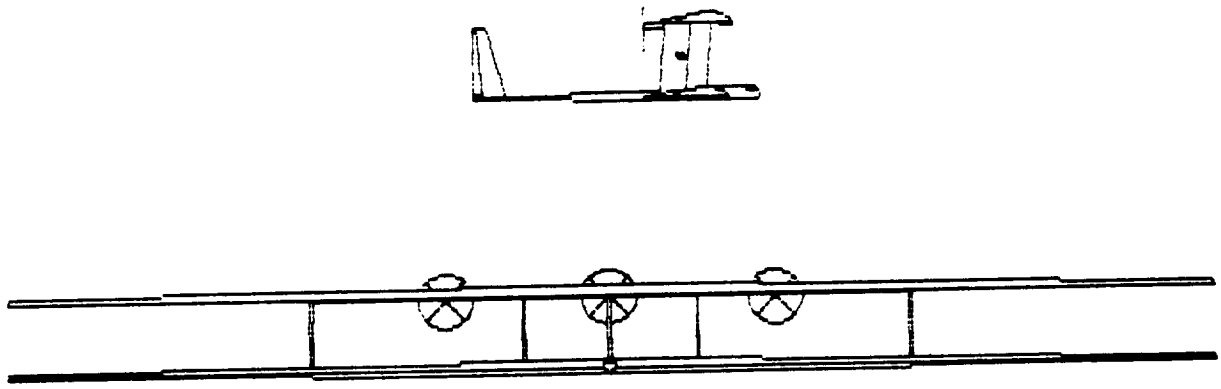

FIGURE 1.6

3.0 FINAL DESIGN

As stated in section 2; a biplane configuration was chosen for the aircraft. The aircraft was thus named the HI-BI, which stands for High altitude BIplane. The aircraft has a twin boom fuselage to minimize the stress at the wing roots. The aircraft has engines mounted on the top wing for maximum propeller clearance. The engines would be aft mounted with pusher propellers to assure uninterrupted flow over the main wings. If tractor propellers were used in front of the wing, the propeller wash would cause aerodynamic interference. The aircraft would have a center fuselage housing the pilot as well as the nose gear, and the payload would be mounted in the lower wing for easy access. For stability and control, the aircraft would have a single horizontal tail joining the two fuselage booms as well as twin vertical tails. The HI-BI aircraft is shown in Figure 3.1.

3.1 PRELIMINARY WEIGHT ESTIMATION

In sizing the aircraft, an initial weight estimation was made. Reference 6 was used to determine initial aircraft weight. It uses weights of similar aircraft to estimate a weight to begin the sizing of the aircraft. Later, in the design stage, when the aircraft configuration becomes more detailed, a refined weight estimation can be made. The initial weight estimation for the HI-BI was as follows:

TAKEOFF WEIGHT	42000 lbs
FUEL WEIGHT	16079 lbs
EMPTY WEIGHT	22921 lbs

3.2 WING GEOMETRY

The criteria for designing the wing is high lift and low drag. Trade-off studies were performed to determine the effect of wing geometry on lift. Figures 3.2 and 3.3 show the effect of wing geometry on $C_{L\alpha}$. From these studies, the wing was designed to have a high aspect ratio with little sweep. The upper and lower wings have identical geometry. The wing geometry is listed in table 3.3.

HI-BI RECONNAISSANCE AIRCRAFT

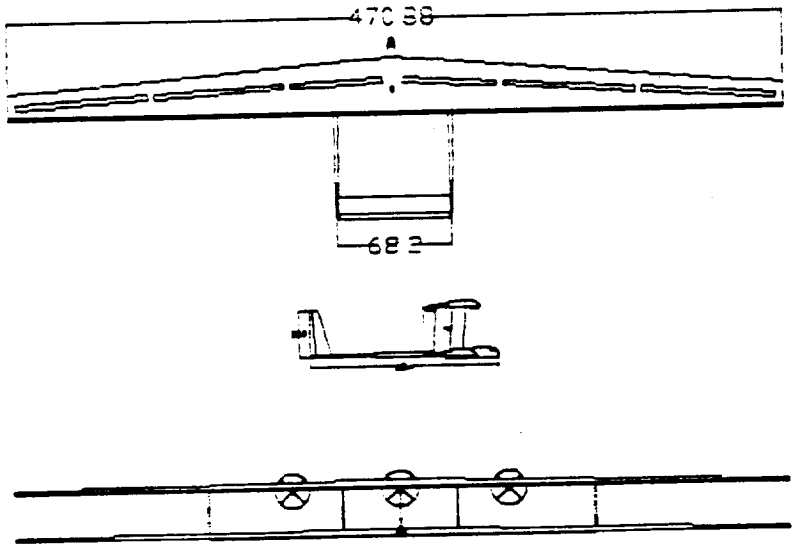

FIGURE 3.1

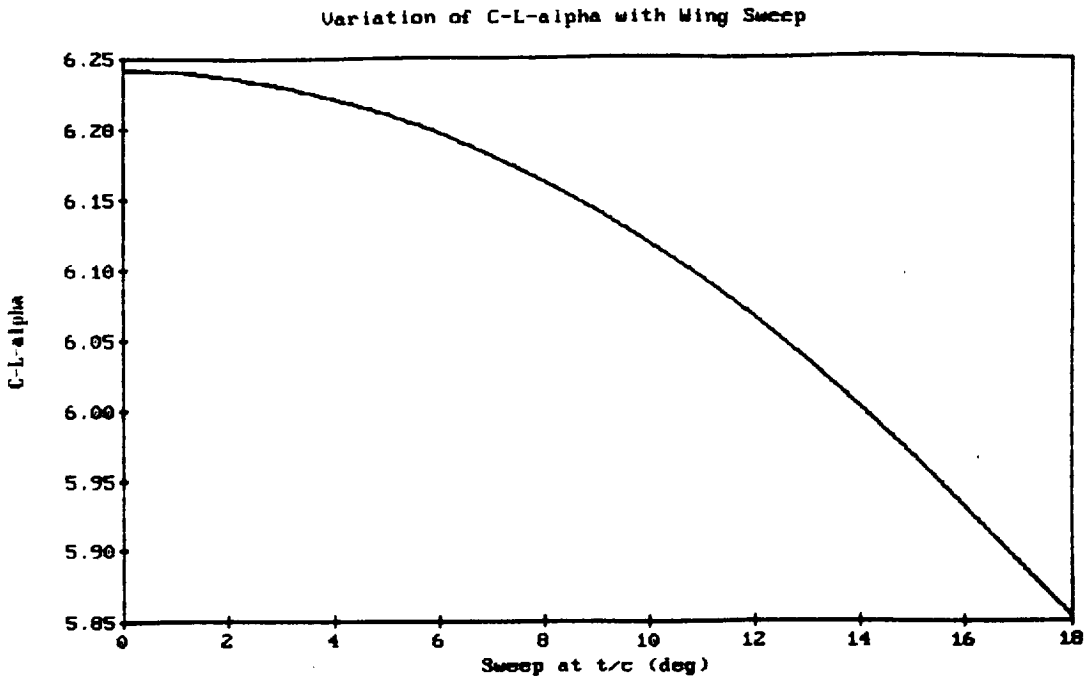

Figure 3.2

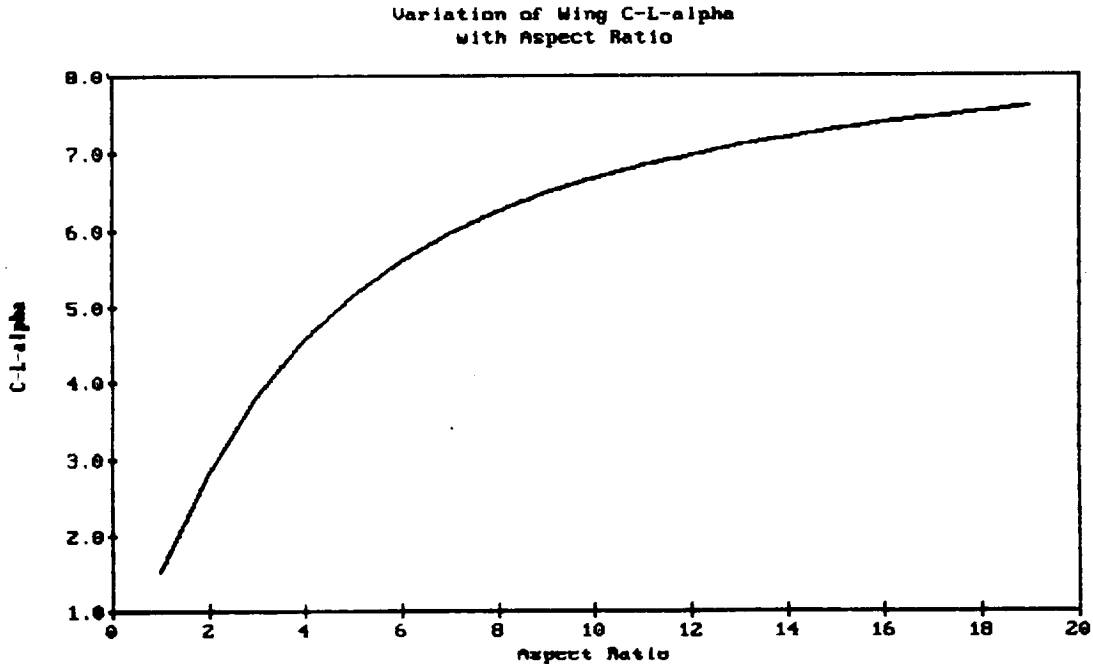

Figure 3.3

From the constraint diagram of Figure 3.4, the wing area per wing was determined to be 11086 ft^2. This corresponds to a wing loading of 1.73. The high aspect ratio wing increases the wing's lift curve slope and reduces the drag due to lift. Because of the large wing area, the aircraft does not need any additional lift during take off and landing. Therefore, the wing has no high lift devices. Ailerons are placed on the lower wing for roll control, and spoilers are placed on the upper surface of the upper wing to reduce the lift during landing.

3.3 HORIZONTAL TAIL

The horizontal tail was sized to trim the aircraft during cruise using the methodology of reference 6. The elevator is used for pitch control. Table 3.3 lists the horizontal tail geometry.

3.4 VERTICAL TAIL

The vertical tail was sized for longitudinal stability and control using the methodology of reference 6. Table 3.3 lists the twin vertical tail's geometry.

3.5 FUSELAGE

The fuselage for the HI-BI consists of a main center fuselage and two fuselage booms. The center fuselage as well as the booms are connected to the lower wing. The

dimension for the fuselage sections are listed in Table 3.1 and Table 3.2

Center Fuselage Dimensions

Average Diameter	3.8 ft
Maximum Diameter	5.9 ft
Body Length	45.3 ft
Body Side Area	170.05 ft^2

Table 3.1

Fuselage Boom Dimensions

Boom Diameter at the Tail	3.1 ft
Boom Diameter at the Wing	1.2 ft
Boom Length*	63.6 ft

* The boom length was measured to be the distance from the wing trailing edge to the aft end of the boom.

Table 3.2

The diameter of the center fuselage at the cockpit area is 4.9 which provides adequate space for a crew of one person. The nose gear is also located in the center fuselage, aft of the cockpit.

3.6 **REFINED WEIGHT ESTIMATION**

After sizing the wing, horizontal tail, vertical tails, and fuselage for the HI-BI aircraft, the method in reference

6 was used to obtain a final weight for the aircraft. The final weight for the HI-BI was:

TAKE-OFF WEIGHT	40622 lbs
FUEL WEIGHT	14573 lbs
EMPTY WEIGHT	22799 lbs

Table 3.4 list the individual component weights for the aircraft. The engine weight listed in the Table includes the weight of the turbochargers.

HI-BI PLANFORM GEOMETRY

	WINGS	HORIZ. TAIL	VERT. TAILS
AREA (ft^2)	11059	924	323
SPAN (ft)	471	68	31
ASPECT RATIO	20	5	3
ROOT CHORD (ft)	34	14	15
TIP CHORD (ft)	13	14	6
LEADING EDGE SWEEP	5	0	16
DIHEDRAL	0	0	-
c-bar	25	14	11

TABLE 3.3

3.7 **MOMENTS OF INERTIA**

The moments of inertia for the HI-BI were determined using the methodology of Reference 9. The moments of inertia of the aircraft are as follows:

$I_{xx} = 10800 \text{ slug-ft}^2$

$I_{yy} = 10500 \text{ slug-ft}^2$

$I_{zz} = 12500 \text{ slug-ft}^2$

HI-BI COMPONENT WEIGHTS

COMPONENT	LBS
WING - 2	5051 per
VERT. TAIL - 2	314.9 per
HORZ. TAIL	480.9
FUSELAGE & BOOMS	717.8
LANDING GEAR	1521.5
ENGINES - 3	1975 per
START SYSTEM	138.1
ENGINE CONTROL SYSTEM	222.4
PROPELLER - 3	571.3 per
PROPELLER CONTROL SYSTEM	172.2
FUEL	14573.3
FUEL SYSTEM	658.1
ELECTRONICS	100
INSTRUMENTATION	49.16
FURNISHING	100.1
AIR CONDITIONING	83.2
CREW	250
PAYLOAD	3000

TABLE 3.4

3.8 CENTER OF GRAVITY LOCATION

Using Reference 6, the center of gravity location was determined for the aircraft. Figure 3.5 shows a side view of the HI-BI with the location of the center of gravity at the take-off weight and at the empty weight. The center of gravity travel between the two extreme conditions is .0747 times c-bar.

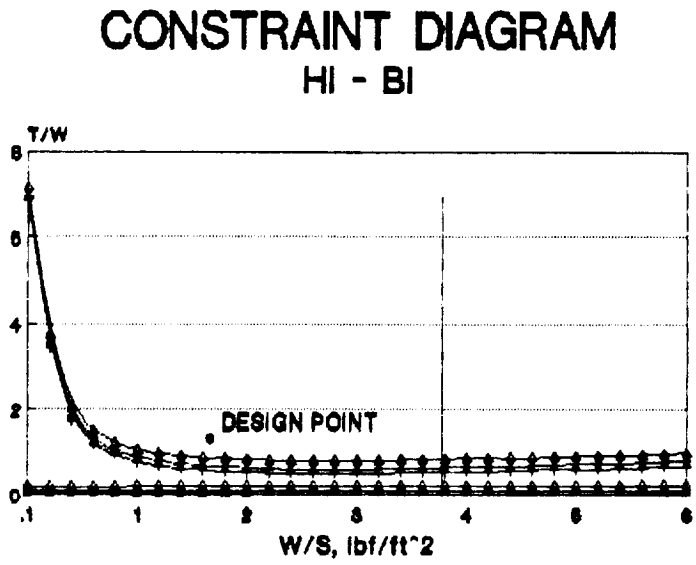

FIGURE 3.4

HI-BI C.G. LOCATION AND TRAVEL

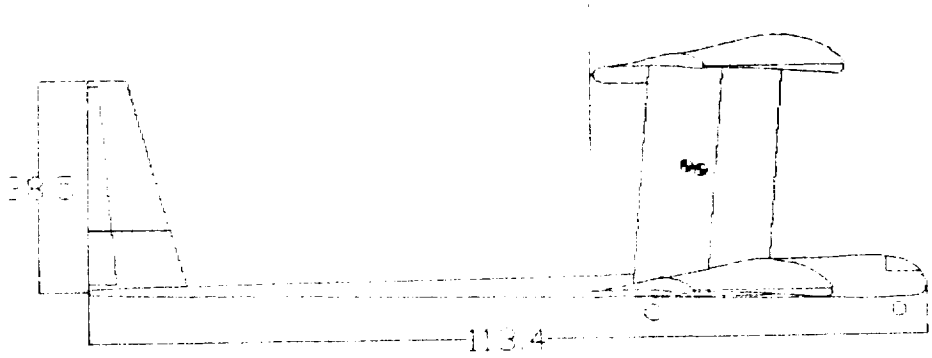

FIGURE 3.5

4.0 AERODYNAMICS

The geometric references used in the aerodynamic calculations for the HI-BI are as follows:

* S_{ref} = 11058.6 ft^2
* MAC = 24.984 ft
* b = 470.88 ft

The reference area used for the aerodynamic calculations is the area of one wing.

4.1 AIRFOIL SELECTION

The criteria used for selection of the airfoil for the HI-BI aircraft was as follows.

* low Reynolds number at altitude
* low drag at cruise
* low pitching moment at cruise
* high c_l

Because of the low air density at cruise altitude, the wing will be operating at a Reynolds number of 500000, and a majority of the flow over the wing surface will be laminar. For flow at low Reynolds numbers, a laminar separation "bubble" will develop on the upper leading surface of the airfoil (Reference 3). If the bubble burst, the flow will separate from the upper surface and lift will be lost. The airfoil should be designed for low Reynolds number flow.

Figure 4.1 shows the variation of skin friction with Reynolds number. Skin friction drag is inversely proportional to Reynolds number. Because the HI-BI wing will be cruising at a low Reynolds number, the zero lift drag will increase. This is an undesirable quality because it increases the powered required for the aircraft.

Low pitching moment is desired in order to decrease the induced drag due by trimming the aircraft.

The airfoil selected to fulfill the requirements is the Liebeck LNV109A airfoil and is shown in Figure 4.2. The LNV109A airfoil has the following characteristics (Reference 3):

* $C_{lmax} = 1.8$
* $C_{l\alpha} = 6.207$ per radian
* $c_{mc/4} = -.05$
* RN > 300000

The LNV109A airfoil is designed for low Reynolds number operation. The LNV109A airfoil also has relatively constant drag coefficient over a large range of lift coefficient. The airfoil drag coefficient is approximately 0.01 over a lift coefficient range of 0.4 to 1.35.

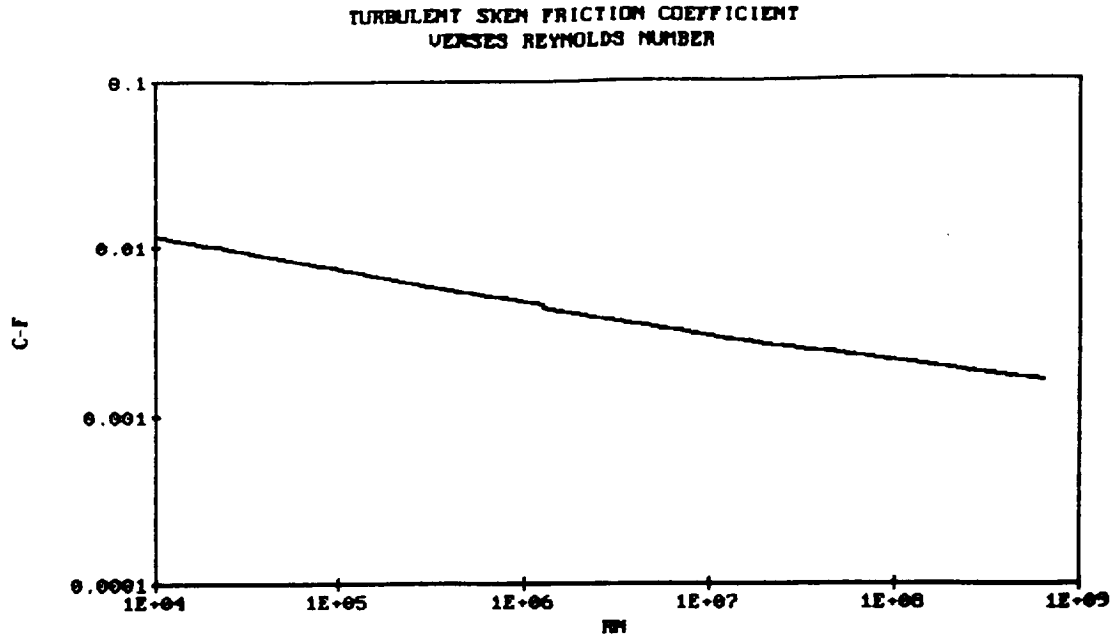

Figure 4.1

LNV109A AIRFOIL FOR HI-BI

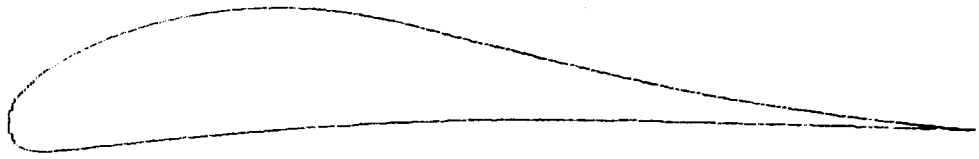

$t/c = 13\%$

Figure 4.2

4.2 LIFT

The lift for the HI-BI is generated by the biplane wings. The lift of the biplane was determined using the methodology in Reference 9, modified for a biplane. The mission requirement dictated the aircraft was to cruise at a constant altitude of 130,000 feet. At the beginning of the cruise portion of the mission, the aircraft will be flying at a total airplane lift coefficient of 1.53. At the end of cruise the total airplane lift coefficient is 1.10.

Because of the close proximity of the two main wings, there are interference effects between the two wings for the biplane configuration. The lift generated by a wing in a biplane configuration will be less than if the wing was in a free stream by itself. Reference 7 shows the interference effects between the two wings is negligible for a spacing of the wings of .9 - 1 times the chord length or greater. The wing spacing for the HI-BI aircraft is .9 times the root chord.

The wings on biplane aircraft are usually staggered one chord length with the upper wing forward of the lower wing. This is done to prevent the lower wing from blocking the flow of the upper wing during extremely high angles of attack. Since the HI-BI aircraft will not be flying at large angles of attack, a stagger of .08 times the mean aerodynamic chord was used. The driving parameter for

determination of the stagger was the placement of the c.g. location to assure static stability.

4.3 DRAG

The difficulty of producing thrust at the required cruise altitude of the HI-BI made it necessary for the drag to be a minimum. The drag of the HI-BI was determined using the methodology of Reference 6. Figure 4.3 shows the drag polar for the HI-BI at the cruise altitude of 130000 feet. At the cruise altitude, the aircraft is operating at a C_d of 0.058. For the cruise C_L of 1.53, the HI-BI is operating at a lift to drag ratio of 26.4.

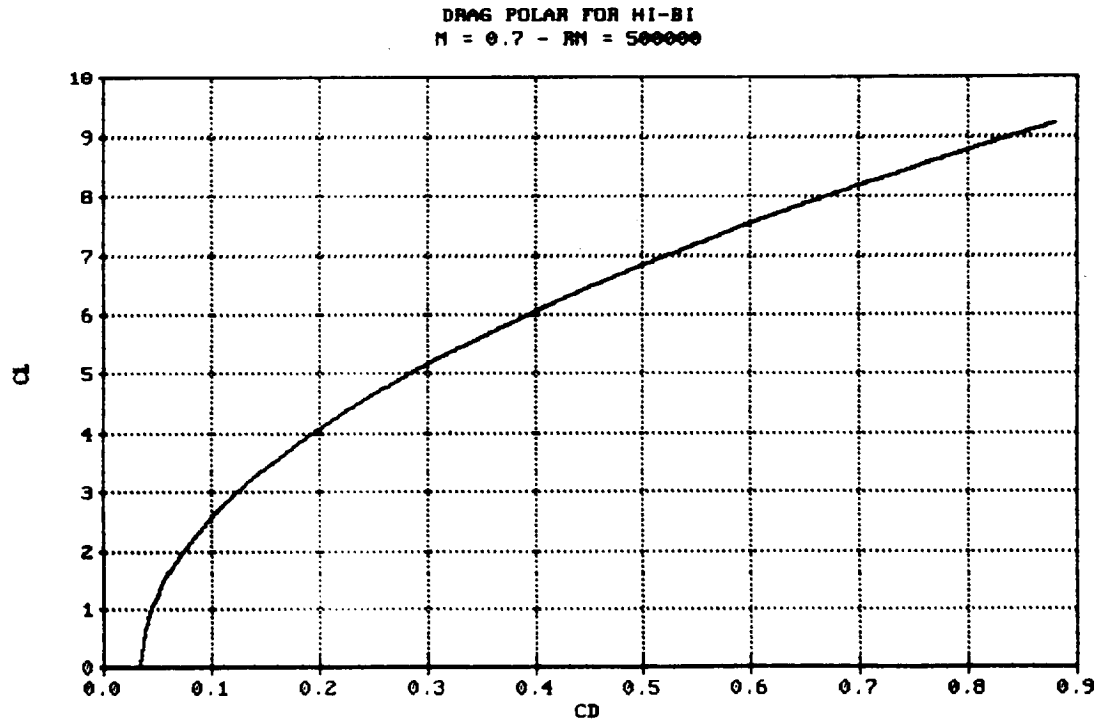

Figure 4.3

5.0 STABILITY AND CONTROL

5.1 STATIC STABILITY

Static stability for the HI-BI aircraft was determined using the methodology of Reference 10. The stability was calculated for four flight conditions (phases) of the mission profile, and the flight conditions are listed in Table 5.1.

MISSION PHASE FOR STABILITY CALCULATIONS

PHASE	ALTITUDE (FT)	VELOCITY (FT/S)	WEIGHT (LBS)
1	0	50	40621.86
2	50K	140	39353.94
3	130K	742.56	38416.7
4	130K	742.56	27485.61

TABLE 5.1

Phase 1 and 2 correspond to velocities for maximum rates of climb during the ascent portion of the mission. Phase 3 corresponds to the beginning of the cruise at altitude, and phase 4 corresponds to the end of the cruise at altitude. Table 5.2 lists the longitudinal stability derivatives for the 4 flight phases. Table 5.3 list the laterial-directional stability derivatives. The HI-BI aircraft is statically stable at the four phases of the flight mission (Reference 9).

LONGITUDINAL STABILITY DERIVATIVES

STABILITY DERIVATIVE	PHASE 1	2	3	4
C-D-alpha	0.5608	0.4565	0.9339	0.6682
C-D-u	0	0	0	0
C-L-i-h	0.3303	0.3324	0.4056	0.4058
C-M-i-H	-0.997	-1.0033	-1.2249	-1.1957
C-L-alpha	11.4296	11.5267	15.2943	15.2943
C-L-U	0.0025	0.0213	1.4784	1.0578
C-L-q	8.3056	8.3734	10.9726	8.7318
C-L-delta-E	0.1569	0.1579	0.1928	0.1928
C-L-alpha-dot	0.8128	0.8251	1.3432	1.3111
C-m-alpha	-1.4371	-1.4405	-1.4822	-0.381
C-m-q	-7.9264	-7.9825	-10.03471	-9.2078
C-m-delta-E	-0.4736	-0.4766	-0.5818	-0.568
C-m-alpha-dot	-2.4535	-2.4905	-4.0543	-3.8631

TABLE 5.2

5.2 DYNAMIC STABILITY

Dynamic stability was done for phase 3 and phase 4 using Reference 9 in conjunction with Reference 14. The dynamic stability was done for these two conditions in order to determine the effect the center of gravity travel had on dynamic stability. Table 5.4 shows the roots of the characteristic equation for the longitudinal perturbation equations of motion for the two phases. The aircraft is dynamically stable about the longitudinal axis. Table 5.5

shows the roots of the characteristic equation for the laterial-directional perturbation equations of motion. The HI-BI is also dynamically laterial-directionally stable.

LATERIAL-DIRECTIONAL STABILITY DERIVATIVES

STABILITY DERIVATIVE	phase 1	2	3	4
C-y-beta	-0.1361	-0.1361	-0.1361	-0.1361
C-y-p	0.0042	0.0038	0.0041	0.0036
C-y-r	0.0423	0.0425	0.0424	0.0415
C-y-delta-R	0.0281	0.0282	0.0339	0.0339
C-l-beta	-0.0577	-0.0886	-0.1793	-0.1654
C-l-p	-0.6135	-0.6194	-0.8195	-0.8195
C-l-r	0.3669	0.3669	0.3669	0.3669
C-l-delta-A	0.2135	0.2156	0.2989	0.2989
C-l-delta-R	-0.0009	-0.0008	-0.001	-0.0009
C-n-beta	0.021	0.0211	0.0211	0.0207
C-n-p	-0.1725	-0.139	-0.2012	-0.144
C-n-r	-0.053	-0.0442	-0.0669	-0.0475
C-n-delta-A	-0.0132	-0.0107	-0.0229	-0.0164
C-n-delta-R	-0.0044	-0.0045	-0.0054	-0.0052

TABLE 5.3

LONGITUDINAL ROOTS OF CHAR. EQU.

PHASE 3

S1,S2 = -.00295 +- j.08149 S3,S4 = -.92065 +- j2.88372

PHASE 4

S1,S2 = -.00292 +- j.1028 S3,S4 = -.95613 +- j1.36055

TABLE 5.4

LATERIAL-DIRECTIONAL ROOTS OF CHAR. EQU.

PHASE 3		
S1 = -.00344	S2 = -25.3165	S3,S4 = -2.542 +- j.68713
PHASE 4		
S1,S2 = -1.752 +- j1.431	S3 = -.000275	S4 = -26.306

TABLE 5.5

5.3 **FLYING QUALITIES**

From Reference 5, MIL-F-8785B, the flying qualities for the HI-BI aircraft can be evaluated. Table 5.6 list the short period and phugoid frequency and damping ratio for phase 3 and 4 for the aircraft. The flying qualities for the short period and phugoid were determined to be level two. This means the flying qualities are adequate to accomplish the mission but with some increase in pilot work load.

Table 5.7 list the spiral and roll time constants and the Dutch roll frequency and damping ratio for aircraft for the two flight phases. The flying qualities were found to be level one for the two flights conditions. This means the flying qualities are clearly adequate for the mission.

Longitudinal Dynamic Response

PHASE 3			
zetaSP = .304	wnSP = 3.03	zetaph = .0362	wnph = .082
PHASE 4			
zetaSP = .304	wnSP = 3.03	zetaph = .036	wnph = .082

TABLE 5.6

Lateral Dynamic Response

PHASE 3			
Ts = .0395	TR = 290.7	zetaD = .965	wnD = 2.63
PHASE 4			
Ts = .0380	TR = 3626.7	zetaD = .775	wnD = 2.26

TABLE 5.7

Figures 5.1 thru 5.6 show the aircraft's response to unit step elevator deflections for the flight conditions of phase 3 and phase 4. Comparing the plots for the two flight conditions, the aircraft's response to elevator deflections become less stable as the aircraft burns fuel (weight decreases). The plane is still stable, but the time responses increase and the overshoots become larger.

Figures 5.7 thru 5.10 show the aircraft's response to unit step aileron deflections for the flight conditions of phase 3 and phase 4. Comparing the plots for the two flight conditions, the aircraft's response to aileron deflections become less stable as the aircraft burns fuel. Again, the plane is still stable, but the time responses increase and the overshoots become larger.

VELOCITY CHANGE FOR UNIT STEP ELEVATOR DEFLECTION
PHASE 3

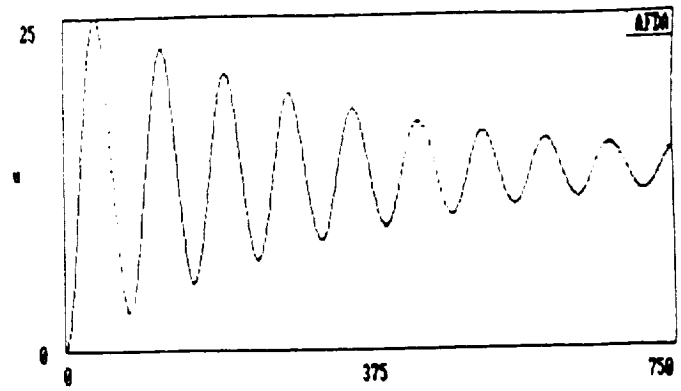

FIGURE 5.1

ALPHA CHANGE FOR UNIT STEP ELEVATOR DEFLECTION
PHASE 3

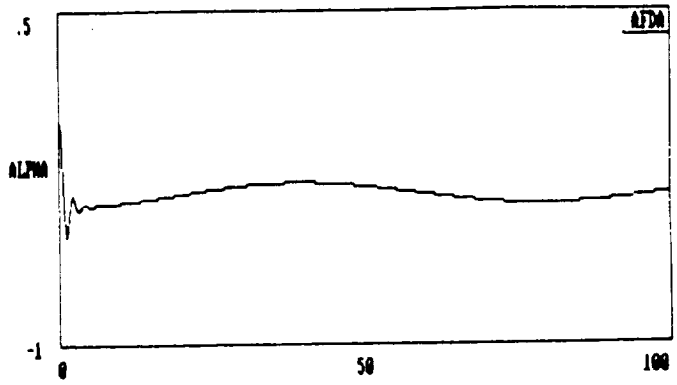

FIGURE 5.2

PITCH ANGLE CHANGE FOR UNIT STEP ELEVATOR DEFLECTION
PHASE 3

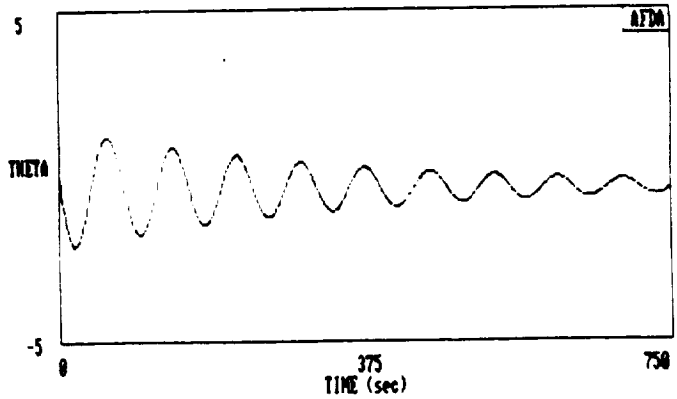

FIGURE 5.3

VELOCITY CHANGE FOR UNIT STEP ELEVATOR DEFLECTION
PHASE 4

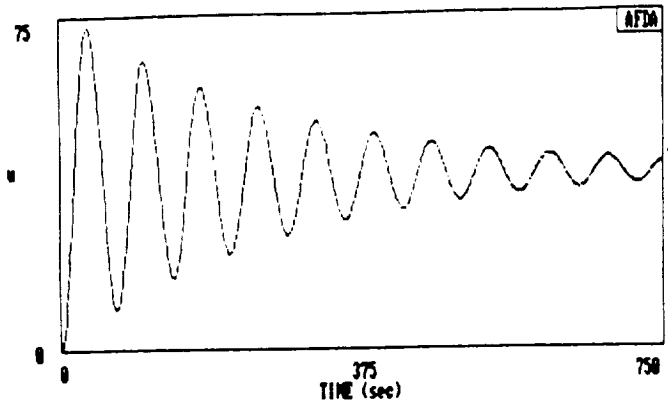

FIGURE 5.4

ALPHA CHANGE FOR UNIT STEP ELEVATOR DEFLECTION
PHASE 4

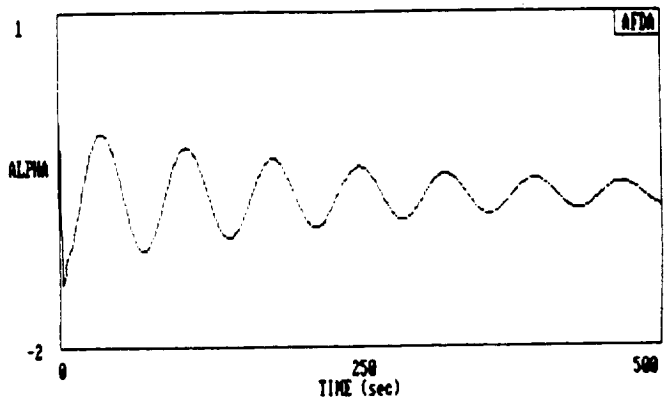

FIGURE 5.5

PITCH ANGLE CHANGE FOR UNIT STEP ELEVATOR DEFLECTION
PHASE 4

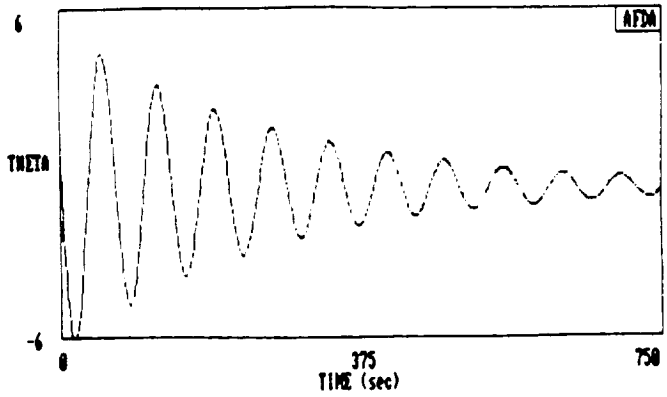

FIGURE 5.6

BETA CHANGE FOR UNIT STEP AILERON DEFLECTION
PHASE 3

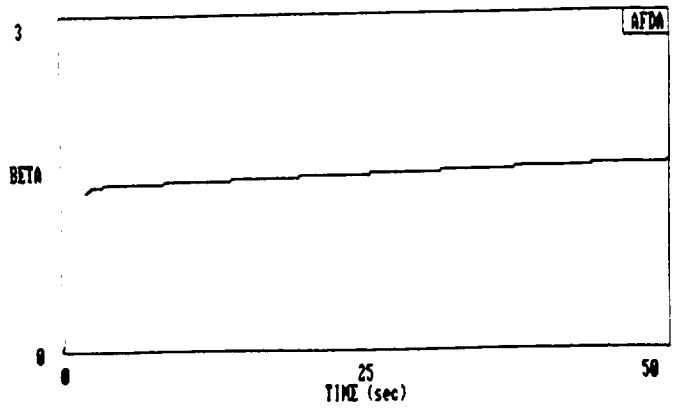

FIGURE 5.7

ROLL ANGLE CHANGE FOR UNIT STEP AILERON DEFLECTION
PHASE 3

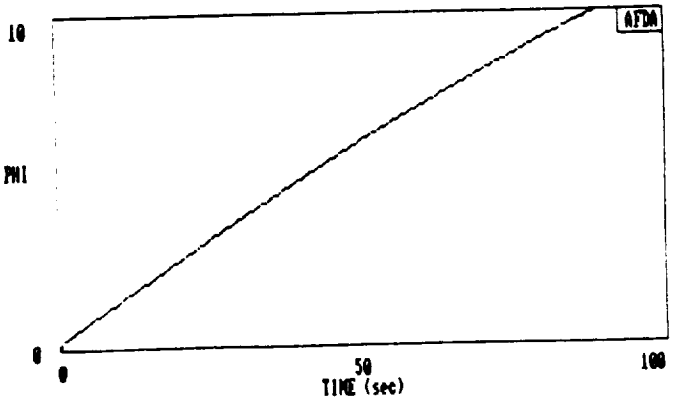

FIGURE 5.8

BETA CHANGE FOR UNIT STEP AILERON DEFLECTION
PHASE 3

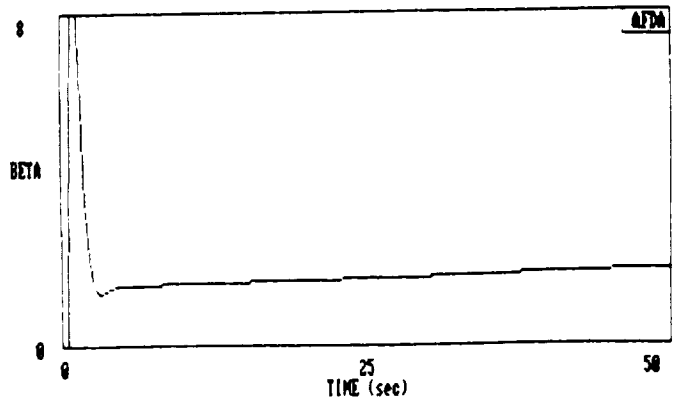

FIGURE 5.9

ROLL ANGLE CHANGE FOR UNIT STEP AILERON DEFLECTION
PHASE 3

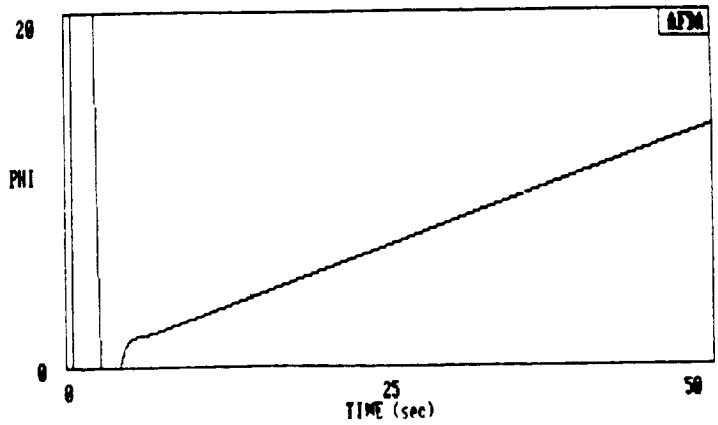

FIGURE 5.10

6.0 PROPULSION SYSTEM

The propulsion system requirements, selection, specifications, and performance will be described in the following sections.

6.1 SYSTEM REQUIREMENTS

The mission profile for this aircraft sets very stringent requirements for the propulsion system. At the operational altitude of 130,000 ft., ambient pressure is approximately 0.3% of standard sea level pressure. The required 0.7 Mach cruise at altitude yields a condition of low mass flow per unit area. In light of these conditions, the powerplant for this aircraft must be able to operate without large quantities of air, low specific air consumption. The 6,000 mile range requirement necessitates that the powerplants have a low specific fuel consumption to reduce the amount and weight of the fuel needed to complete the mission.

Since the aircraft is to operate at subsonic velocities and very high altitudes, the aircraft's wings will be large and heavy. This will require an engine that is capable of producing large amounts of power at altitude. The final requirements are to keep the engine and its systems as light as possible and to develop this system with current technology.

Figure 6.1 tabulates the requirements for the high altitude propulsion system.

Figure 6.1

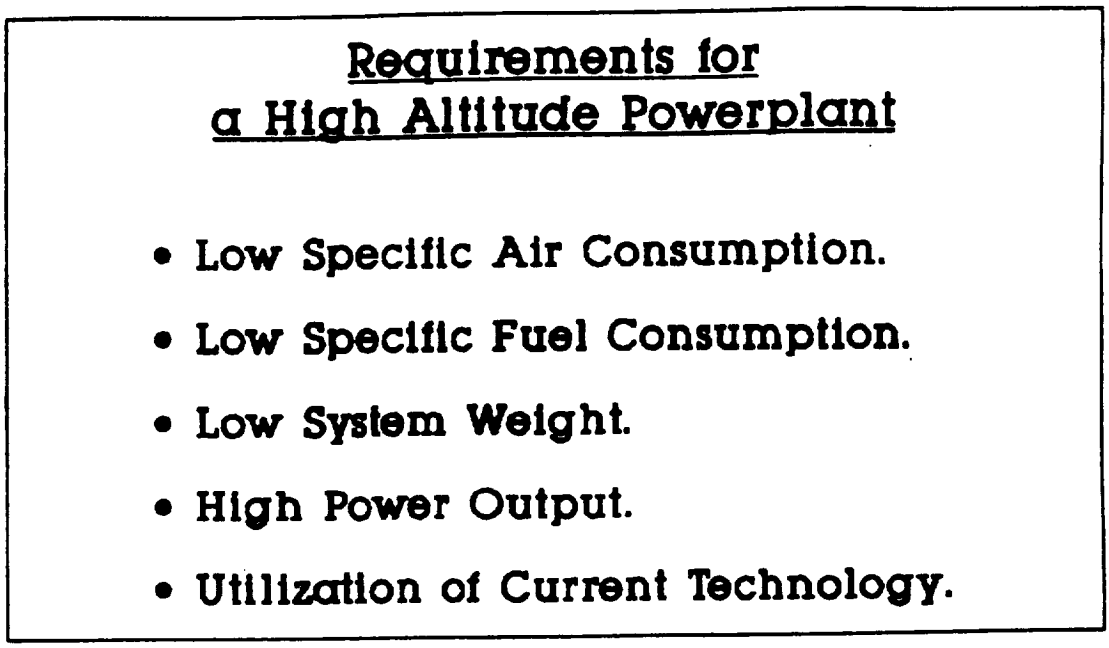

6.2 POWERPLANT SELECTION

Various engines were evaluated for their ability to satisfy the requirements for a high altitude propulsion system. The driving constraint in the engine selection process was the air consumption of the engine at altitude. The air consumption had to be low for the engine to produce power at altitude. Figure 6.2 shows typical specific air consumption (SAC) values for the engines examined. The second constraint was propulsion system weight. The system weight is the weight of the engine and weight of the fuel required for the mission.This had to be kept as low as possible. Figures 6.3-6.4 show typical specific fuel consumption (SFC) and specific weight values for the engines examined. The engines evaluated for this aircraft are described in the following sub-sections.

Figure 6.2

Specific Air Consumption for Various Engine Types

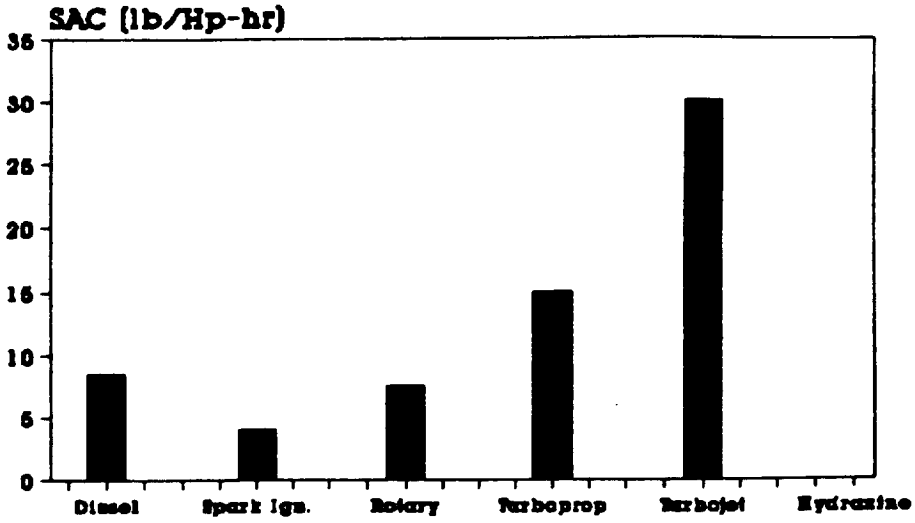

Figure 6.3

Specific Fuel Consumption for Various Engine Types

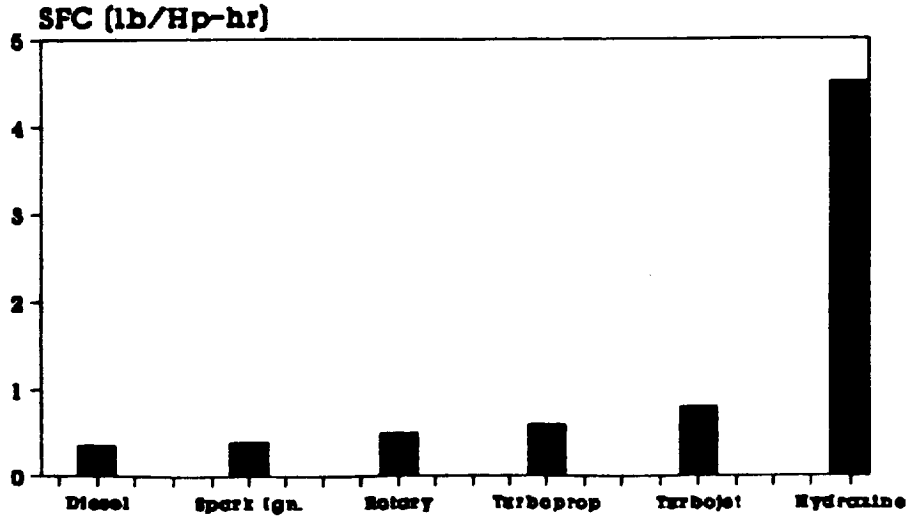

Figure 6.4

Specific Weight
for Various Engine Types

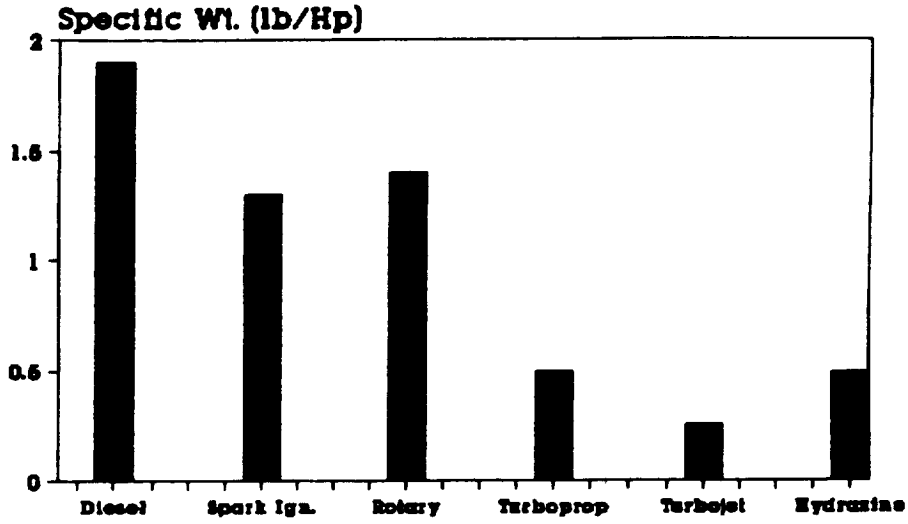

6.2.1 TURBOJETS/TURBOFANS

The use of turbojets or turbofans to complete the high altitude mission was first evaluated. The Pratt & Whitney J75 turbojet, the engine used on the U-2 and the TR-1, was the engine selected for examination. Figure 6.5 shows the performance of the engine with altitude. The J75's thrust goes from 17,000 lb. static sea level thrust to approximately 50 lb. of thrust at the cruise altitude of 130,000 ft.

The low density of the air at altitude and subsonic cruise velocity combined with the engine's high specific air consumption, make it impossible for any turbojet or turbofan engine to produce any meaningful thrust.

Figure 6.5

Thrust vs. Altitude
for a 17000 lb Thrust Turbojet

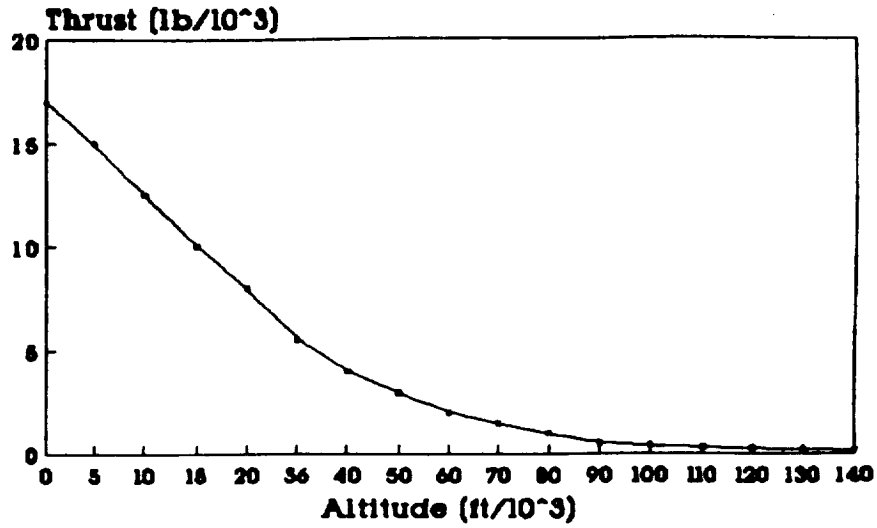

6.2.2 TURBOPROPS

After deciding that turbojets/turboprops were not feasible, attention was turned towards turboprops. Turboprops produce shaft power instead of accelerating air for thrust and have half the SAC of turbojets. However, turboprop engines still require more air than is available at altitude. Therefore, they follow the same power trend as the turbojet, Figure 6.5, producing little power at altitude.

6.2.3 HYDRAZINE ENGINE

The hydrazine monopropellant reciprocating engine was evaluated as a possible powerplant for the high altitude aircraft. This type of engine uses hydrazine as a fuel and does not require ambient air for combustion. The hydrazine

engine was developed by NASA for the Mini-Sniffer high altitude aircraft, Reference 15. The engine for the Mini-Sniffer generated 15 Hp. An engine for this aircraft would be a scaled up version of the Mini-Sniffer engine.

The hydrazine engine has an extremely high specific fuel consumption, Figure 6.3, compared to other types of engines. Hydrazine is also a toxic substance and must be specially handled. Despite these drawbacks, the hydrazine engine was considered for further study.

6.2.4 INTERNAL COMBUSTION ENGINES

Attention was given to exploring the feasibility of using internal combustion (IC) engines for a high altitude powerplant. IC engines have a relatively low SAC of 5-10 lb/Hp-hr. The fuel consumption of these types of engines are also attractively low, 0.3-0.5 lb/Hp-hr. Although these engines have a low SAC, they would be unable to produce enough power at altitude without some type of supercharging. The Lockheed HAARP Project, Reference 25, designed a turbocharging system to operate with an IC engine at an altitude of 100,000 ft. It was felt that such a system could also be designed for the required altitude of 130,000 ft.

A major drawback to IC engines is their high specific weight, Figure 6.4. The high specific weight of these engines added with the weight of the required turbocharging system will result in a propulsion system would be extremely heavy.

Of the three IC engines examined, diesel, rotary, and spark ignition, the spark ignition engine had the best mix of SAC, SFC, and specific weight. The spark ignition IC engine was selected for further study.

6.2.5 OTHER TYPES OF POWERPLANTS

Other engine technologies such as microwave propulsion, laser propulsion, nuclear propulsion, and electrical propulsion were examined. Practical versions of engines were not feasible with present day technology and received no further consideration.

6.2.6 SELECTION OF THE POWERPLANT

The two types of engines selected for further study were the hydrazine monopropellant reciprocating engine and the spark ignition reciprocating engine. Both engines were capable of operating at the required altitude of 130,000 ft and developing at least 500 Hp when scaled up. A system weight study was conducted to determine which of the engines would incur the least weight penalty completing a ten hour mission. Figure 6.6 shows the results of this study with both engines configured for operation at 130,000 ft.

The weight study showed that the spark ignition propulsion system was four times lighter than the hydrazine system. The main difference between the two engines is the fuel required for the ten hour mission.

Figure 6.6

Compairison of Estimated Total Propulsion Weight

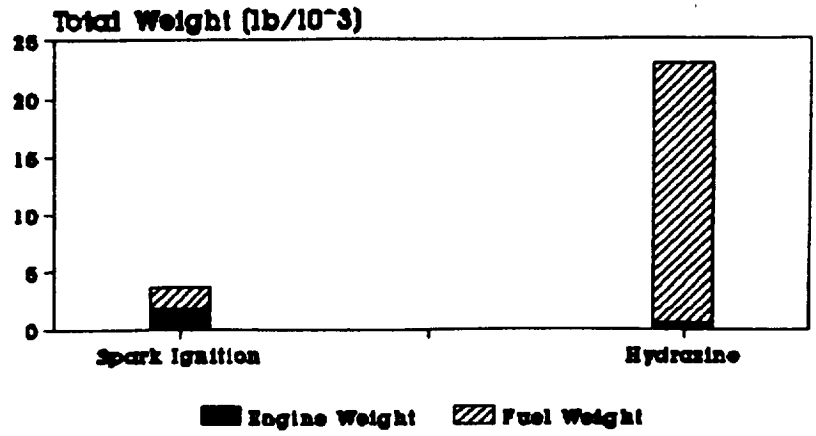

Note: 10 hour mission
600 Hp engine
Equipped for 130,000 ft.

Figure 6.7

Powerplant Configuration

- Reciprocating Spark Ignition.
- Horizontal Opposed Cylinders.
- Four Stage Turbocharged.
- Fuel Injected.
- Dual Ignition.
- Liquid Cooled.
- Geared Propeller Drive.

Thus, the spark ignition IC engine was selected as the best choice for the high altitude propulsion system.

6.3 ENGINE CONFIGURATION

The configuration and details of the IC spark ignition engine developed for this project will be set forth in the following sub-sections. The engine configuration is shown in Figure 6.7.

6.3.1 TURBOCHARGING SYSTEM

The high altitude engine uses four stages of turbocharging to allow it to operate at altitude. Turbocharging was selected over supercharging so that the engine power would not have to be used. Figure 6.8 shows a schematic of the turbocharging system. Figure 6.9 tabulates the specifications of the system. The turbochargers are each composed of a radial compressor and a radial turbine. Each of the four turbocharger stages are intercooled with a crossflow air to air heat exchanger.

The full compression capacity of the system is only required at the cruise altitude. The pressure in the system is controlled by a waste gate installed between the engine and the high pressure turbine, Figure 6.8. The waste gate is designed to dump all exhaust up to a density altitude of 2800 ft. From 2800 ft. density altitude, the waste gate closes with the decrease in density. Full closure of the waste gate occurs

at a density altitude of 97,000 ft. As an added safety measure, an over pressure safety valve is incorporated between the high pressure compressor and the engine.This valve will release pressure if the pressure in the system becomes greater than 2140 psf. This protects the engine from a potentially disasterous over pressure from the turbochargers.

Figure 6.8

Schematic of the Four Stage Turbocharging System

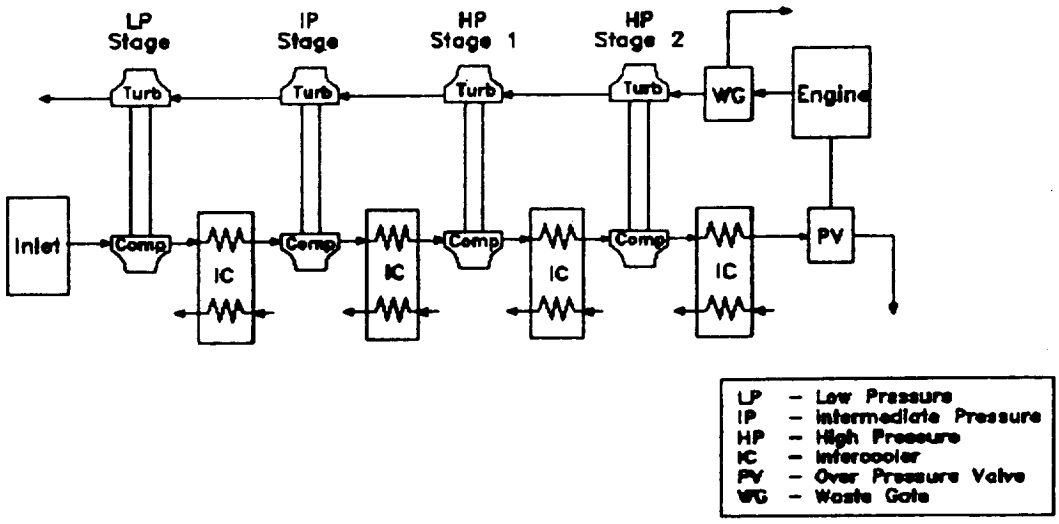

Figure 6.9

Specifications of the Four Stage Turbocharger System

Turbocharger Type	Radial
Over All Pressure Ratio	432:1
1st Stage Pressure Ratio	3:1
2nd Stage Pressure Ratio	4:1
3rd Stage Pressure Ratio	6:1
4th Stage Pressure Ratio	6:1
Maximum Mass Flow Rate	120.5 (lb/min)
Maximum Pressure Obtained at 130,000 ft.	1788 (psia)
Inlet Size	8.7 (ft^2)
System Weight	900 (lb)

6.3.2 ENGINE BLOCK AND CYLINDERS

The high altitude engine is arranged in a horizontal opposed configuration to reduce frontal area and allow an aerodynamic cowling to be fitted around the engine. The block is made up of two forged aluminum alloy pieces bolted together vertically. The crank shaft is a forged steel, eight-throw, one piece design and is supported by five journal bearings.

The engine has eight, 10:1 compression ratio, aluminum alloy pistons displacing 1125 cubic inches. Each cylinder is made up of aluminum structure with a forged steel bore sleeve chrome plated to reduce wear and an aluminum alloy head. The cylinders are bolted separately to the block allowing for single cylinder replacement. There is one intake and one

exhaust valve per cylinder. The valve train is driven by a single camshaft geared to the crank. The valves are connected to the camshaft through a rocker arm-pushrod setup.

6.3.3 LUBRICATION SYSTEM

The lubrication system for the high altitude engine is a pressure feed with a dry sump. The oil is pumped by a positive displacement gear type pump and the full flow is filtered. The oil receives cooling from a heat exchanger mounted in the front of the engine cowling. The oil used by the system is a 20/50 multi-grade.

6.3.4 COOLING SYSTEM

The cooling system used for the high altitude system is a pressurized liquid system. The coolant used is a 60/40 mix of Ethylene Glycol and water pressurized to 14 psig. The system uses a mechanical centrifugal pump capable of delivering 125 gal/min of coolant to the engine. The system has one radiator and a heat sink in the aircraft's fuel cell. The mean temperature of the coolant is 210 F and maximum system temperature is 265 F.

6.3.5 FUEL SYSTEM

The fuel system for the high altitude powerplant consists of a demand type mechanical pump with an electric back-up pump. The fuel pump delivers the fuel to a electronic

metering pump. This pump will vary the fuel inputs to the injectors to keep the correct air fuel ratio. There is one injector per cylinder injecting the fuel into the cylinder during the intake stroke. The fuel used by the system is 100 Low Lead aviation gasoline.

6.3.6 IGNITION SYSTEM

The ignition system for the engine consists of a dual electronic ignition system. Each circuit is totally separate and shielded with its own set of plug wires and plugs.

6.3.7 GEAR REDUCTION

A gear reduction box is employed to reduce the engine RPM down to an acceptable speed for the propeller. The gear reduction box is also used to mount and drive an auxiliary alternator. The gear reduction box has provisions for mounting other engine driven devices.

6.3.8 ELECTRICAL SYSTEM

The electrical system for the high altitude engine consists of a single mechanical 24 volt alternator powering dual 24 volt batteries and the engine sensors and aircraft systems. An extra alternator is driven by the engine to supply power for the payload package.

6.3.9 ENGINE CONTROL SYSTEMS

The engine control system for the high altitude engine is split in two parts, pilot controls and computer controls. The pilot controls the engine through dual throttles and pitch levers. The computer controls the engine's fuel mixture, ignition timing, and turbocharger waste gate to achieve the optimum performance.

The information on condition of the engine is displayed to the pilot through RPM gages, oil pressure gages, cylinder head temperatures, coolant temperature, and manifold pressure gages. Any engine faults are recorded by the computer for later retrieval.

6.4 PERFORMANCE SPECIFICATIONS

This section describes the performance of spark ignition engine developed for this aircraft.

The powerplant was modeled on an engine program modified from Reference 19. The program takes design parameters for the engine, preforms a cycle analysis, and outputs the performance of the designed engine. The program simulated the an eight cylinder engine and turbochargers operating at 130,000 ft. Figure 6.10 shows the specifications and performance for the engine designed for this aircraft. Figures 6.11 and 6.12 show cycle information on the engine's pressure vs. volume and heat transfer vs. gas temperature respectively.

Figure 6.10

Performance Specifications
960 Hp Engine

Engine Type	IC Spark Ignition
Number of Cylinders	8
Cylinder Arrangement	Horizontal Opposed
Bore and Stroke	5.25 in and 6.5 in
Displacement	1125 cu in
Compression Ratio	10:1
Width and Height, Engine	38 in and 29.25 in
Width and Height, Installed	41 in and 59.8 in
Length and Frontal Area, Engine	33.6 in and 7.7 sq ft
Length and Frontal Area, Inst.	69.6 in and 16.4 sq ft
Engine Weight	11177 lb
Total Weight, Installed	2077 lb
Weight/Horsepower	1.89 lb/Hp
Fuel Grade	100 LL
SFC, Cruise and Max Power	0.357 and 0.383 lb/Hp-hr
SAC, Cruise and Max Power	5.684 and 5.45 lb/Hp-hr
Cruise Power	962 Hp/3900 RPM • 130k ft.
Max Power	1194.9 Hp/4250RPM • S.L.
	1100 Hp/4250 RPM • 130k ft.

Figure 6.11

Pressure vs. Volume Diagram
960 Hp Engine

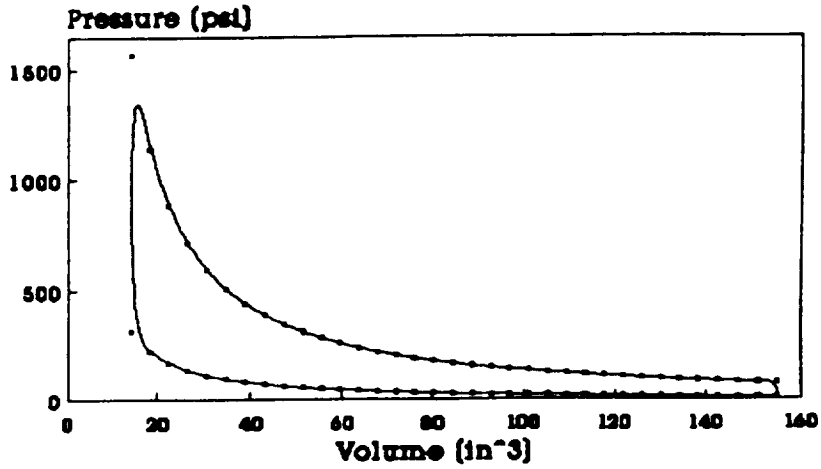

Cruise Conditions
Displacement = 1125 cu.in.

Figure 6.12

Heat Transfer vs. Temperature
960 Hp Engine

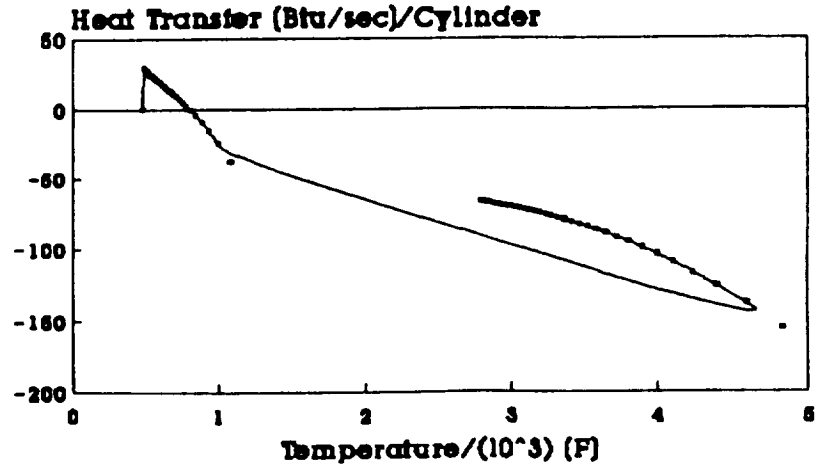

Cruise Conditions
Engine Displacement = 1125 cu.in.

6.5 PROPELLER DESIGN

After analyzing the mission profile, the cruise phase was determined to be the flight phase governing the propeller size. This is due to the fact that the air density is very low at the cruise altitude of 130,000 feet. The two main criteria at cruise for the propellers were:

* Since the air density is low at altitude, the propeller will have to have a large diameter
* The tip velocities can not exceed the local sonic speed because of compressibility effects.

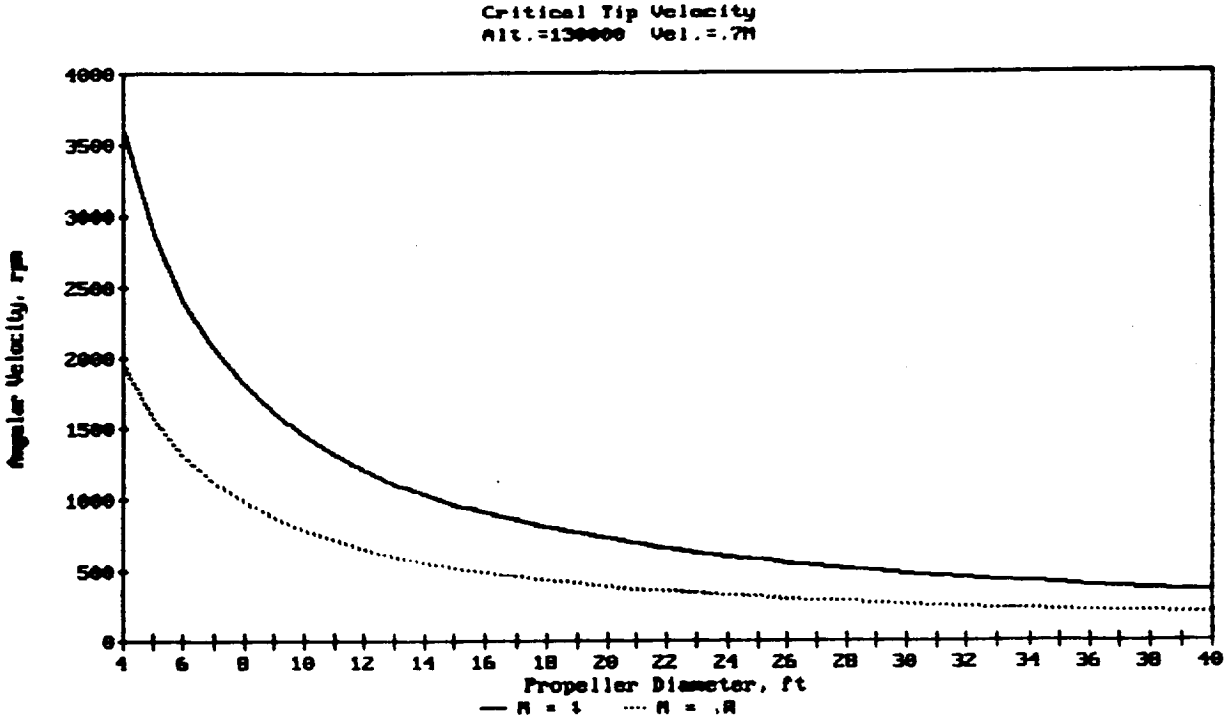

Figure 6.13

Figure 6.13 is a graph of constant tip velocity for M = 1 and M = 0.8 as a function of angular velocity, n, and propeller diameter, D. Any combination of n and D above the M = 1 curve will give tip velocities greater than the local sonic speed. At this altitude, the sonic speed is 1060 fps. In fact, the tip speeds should not exceed a Mach number of 0.8 because local velocities on the blades can go sonic. Therefore, The propeller should operate in the region below the M = 0.8 curve. As can be seen in the figure, this region is very narrow for propeller diameters of over 20 feet.

It was determined that at cruise, the drag was equal to 1708 pounds, which for a constant velocity, is equal to the thrust required. This value of thrust corresponds to 2304 horsepower for a cruise velocity of 742 fps (M = 0.7). Therefore, for the three propellers, each must produce 768 hp.

7.0 PERFORMANCE

7.1 TAKEOFF

The take-off performance for the HI-BI was evaluated using methods outlined in References 4 and 6. The wing loading on takeoff was found to be 3.86 lbs/ft^2 and with the air density and CLmax known , the stalling velocity was determined to be 30.9 fps. This is a very low value for stall velocity due to the low wing loading. Therefore, it was decided to stall the top wing with spoilers in order to increase the wing loading and thus increase Vstall. In so doing, the aircraft will not lose lift due to wind qust. Vstall was increased to 43.7 fps. The take-off velocity Vto is then 1.2 times Vstall and has a value of 52.4 fps. The acceleration is assumed to be constant and taken at .7 times Vto. A force balance on the aircraft was done to get the acceleration. The distance traveled by the aircraft from a zero velocity to Vto was then calculated to be 390 feet. This is the ground roll distance S_G. The distance in which the plane then rotates into take-off position is known as the rotation distance SR and was calculated to be 157.2 feet. Next, the transition distance STR was determined. This is the ground distance that the plane actually travels as it climbs through a constant velocity arc. This distance was equal to 70 ft. and at this point the plane has not cleared an imaginary 50 foot high wall. The distance to

clear this barrier was determined to be 372.3 feet. Therefore, the total take-off distance is equal to 989.5 feet.

When talking about take-off performance, one needs to look at balanced field length. This is the distance needed for the aircraft either to take-off and clear the barrier or brake and come to a stop in case of an engine failure.

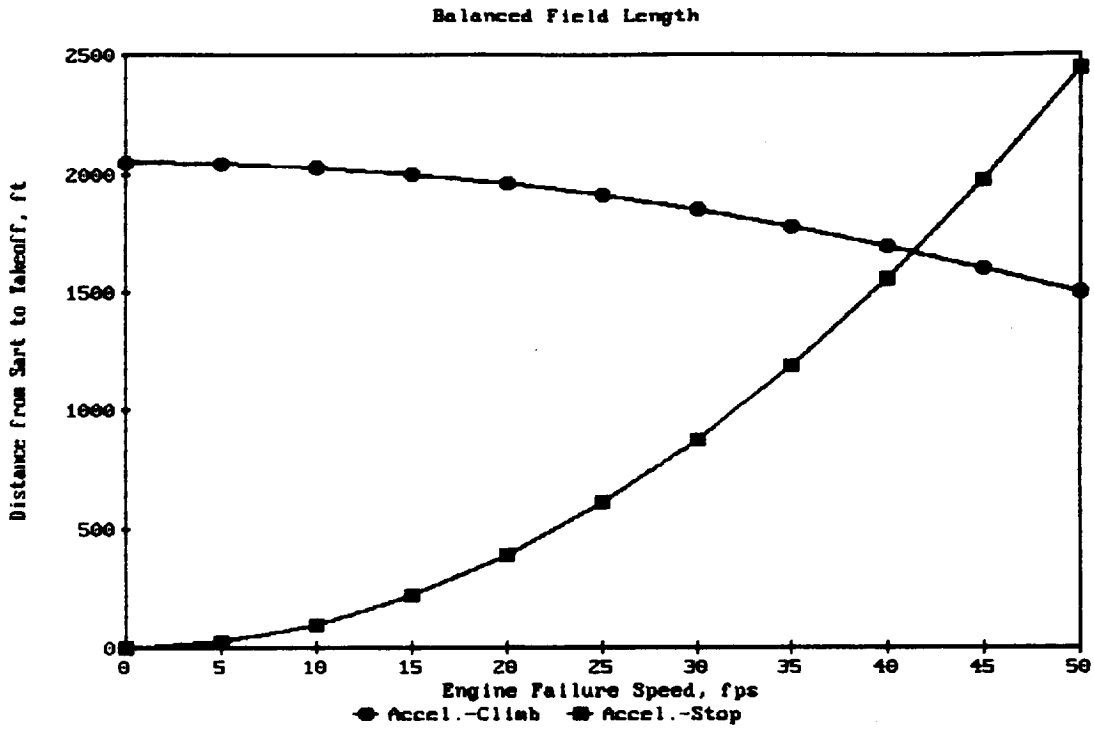

Fig. 7.1

The distance is said to be balanced if at a given velocity, the total distance traveled up through takeoff is equal to the distance, at the same velocity, traveled with one engine

inoperative and the aircraft is brought to rest. From Figure 7.1, the balanced field length is the distance corresponding to the intersection of the two curves. This is read off the plot to be about 1750 feet. The corresponding critical speed, Vcrit, is 43 fps. Therefore, if one engine fails at a velocity higher than 45 fps, the take-off should be continued. If the failure occurs at a lower velocity than Vcrit, The take-off should be aborted.

7.2 Landing

For the landing analysis, the weight was equal to 22748 lbs and a CLmax of 3.6. Thus, Vstall was calculated to be 31 fps. The total landing distance can be thought of the sum of three parts, the Air Distance SA, the Free Roll Distance SFR, and the Braking Distance SB. Using methods outline in Reference 6, SA was found to be 325 feet. This is the horizontal distance that the plane travels after having passed over the 50 foot wall up through touch down. The Free Roll is the distance traveled as the plane's nose pitches down and the front landing gear makes contact. This distance was equal to 106.5 feet. The distance to a complete stop, SB, was found using a braking coefficient of .5. This distance was determined to be 32.3 feet. Thus, the total distance for landing was found to be 463.8 feet. Table 7.1 summarizes the values obtained for the various distances.

TAKE-OFF W/S=3.86 T/W=.199		LANDING W/S=2.05 T/W=0	
Ground roll SG	390 ft.	Air SA	325 ft.
Rotation SR	157.2 ft.	Free Roll SFR	106.5 ft.
Transition STR	70 ft.	Braking SB	32.3 ft.
Climb SCL	372.3 ft.		
TOTAL	989.5 ft.	TOTAL	463.8 ft.

Table 7.1

7.3 **CLIMB**

The climb performance was determined using the methods of Reference 12. The objective of the climb analysis was to minimize the time the HI-BI was required to climb to the specified cruise altitude. Minimizing the time to climb minimized the fuel required to climb to cruise altitude. Figure 7.2 shows plots of the HI-BI's rate of climb as a function of airspeed and altitude. To minimize the time required to climb, the HI-BI's velocity should correspond to the maximum rate of climb at the corresponding altitude. Figure 7.3 shows the maximum rates of climb as a function of velocity taken from Figure 7.2. Using the maximum rates of climb from Figure 7.3, the time to climb to 130000 feet cruise altitude was determined to be 66.2 minutes. Using

the time required to climb, the fuel required to climb to the cruise altitude was determined to be 1330.75 lbs.

7.4 CRUISE

The RFP stated the aircraft was required to either cruise at a 130000 foot altitude for 6 hours or to fly a total mission distance of 6000 miles. The constraining factor to determine the cruise distance was the 6000 miles total mission distance. The HI-BI was determined to cruise at altitude for 10.9 hours. A Mach 0.7, this corresponds to a cruise distance of 5519.6 miles.

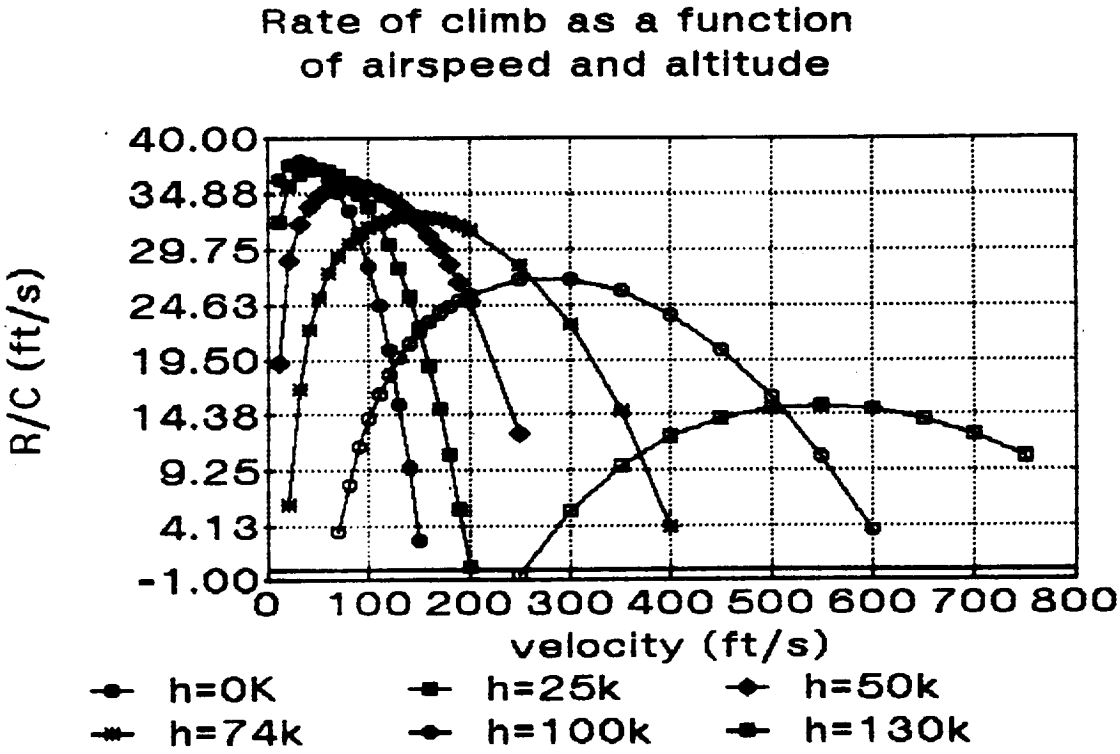

FIGURE 7.2

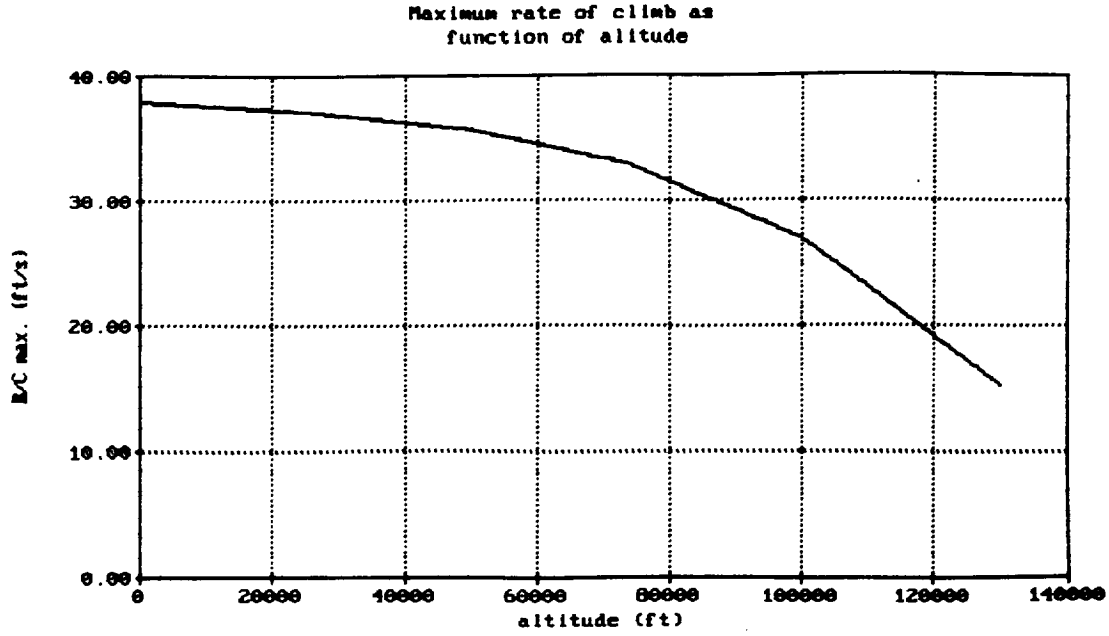

FIGURE 7.3

7.5 Flight Envelope

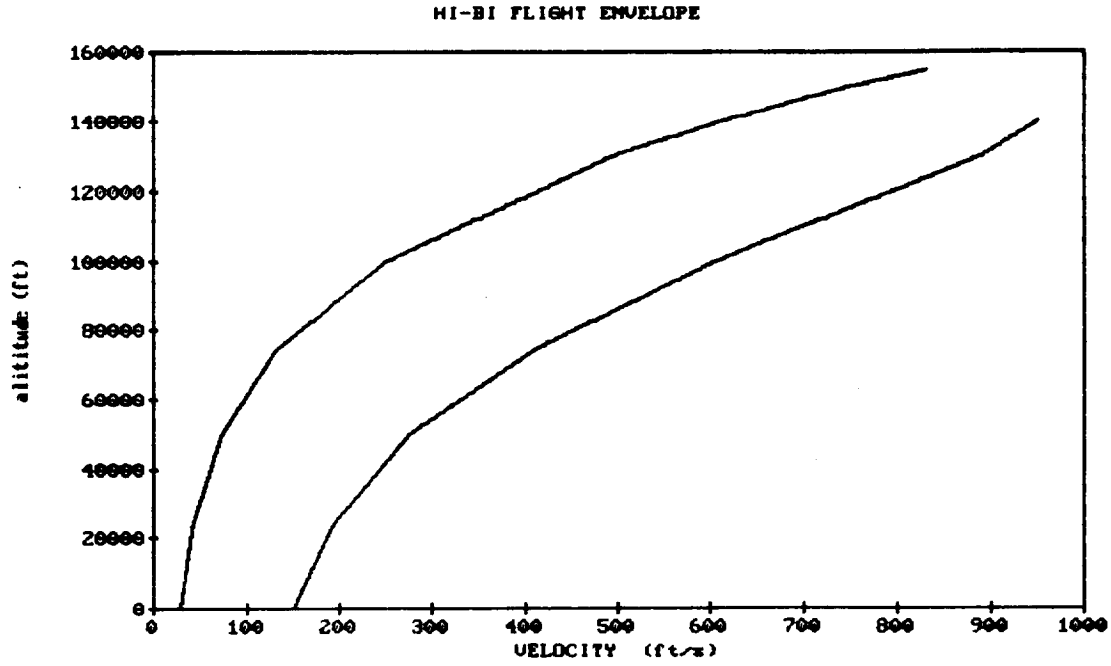

Figure 7.4

The flight envelope in Figure 7.4 was developed using methods outline in Reference 4. A flight envelope is the area on an altitude versus velocity plot where the aircraft can fly. At low speeds, the aircraft is constrained by the stall velocity and at higher speeds the constraint is maximum power. The top curve on the Figure represents stall velocity with increasing altitude. The stall velocities are related to altitude by the following equation:

$$(V_{stall})^2 = (2W/S)/(rho_o C_{Lmax} \sigma)$$

The density ratio σ varies with altitude thus at any given altitude there is a unique V_{stall}. From Figure 7.4, it can be seen that V_{stall} is about 30 fps at sea level and gets to be about 500 fps at 130000 feet altitude. The stall velocity at 130000 feet is well below the operating velocity of 742 fps.

The maximum power curve also increases with altitude and follows the stall curve closely. This gives a flight envelope that is somewhat narrow. Thus, much care must be taken when piloting HI-BI in order to stay within the flight envelope.

7.6 POWER REQUIRED

Using the drag determined earlier and Reference 6, the power required for the flight mission was determined. Figure 7.5 shows the HI-BI's required power as a function of

velocity and altitude. The Figure shows as the plane increases in velocity and altitude, the power required increases. The cause of the increase in power is the decrease in Reynolds number with increase in altitude. As stated earlier, the drag of the aircraft increases with decrease in Reynolds number. Figure 7.6 shows a plot of Reynolds number as a function of altitude. From Figure 7.5, the power required to cruise at altitude was determined to be 2168.7 hp.

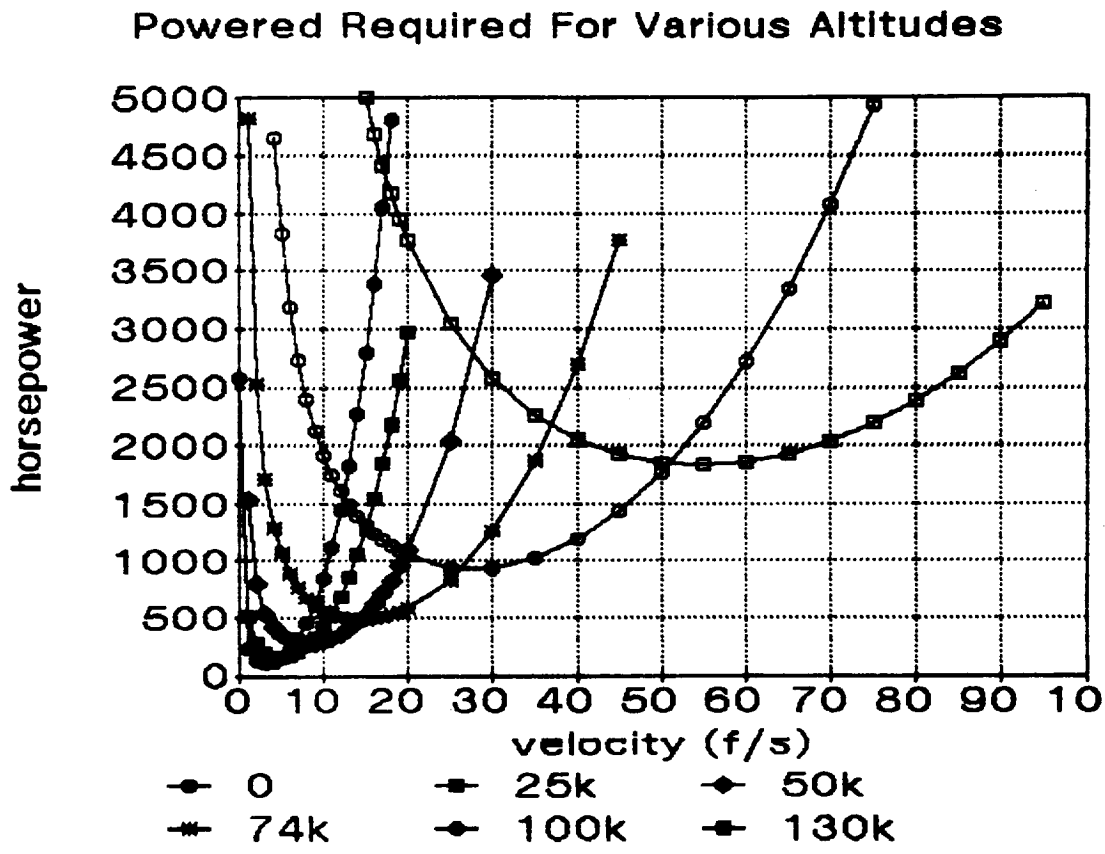

FIGURE 7.5

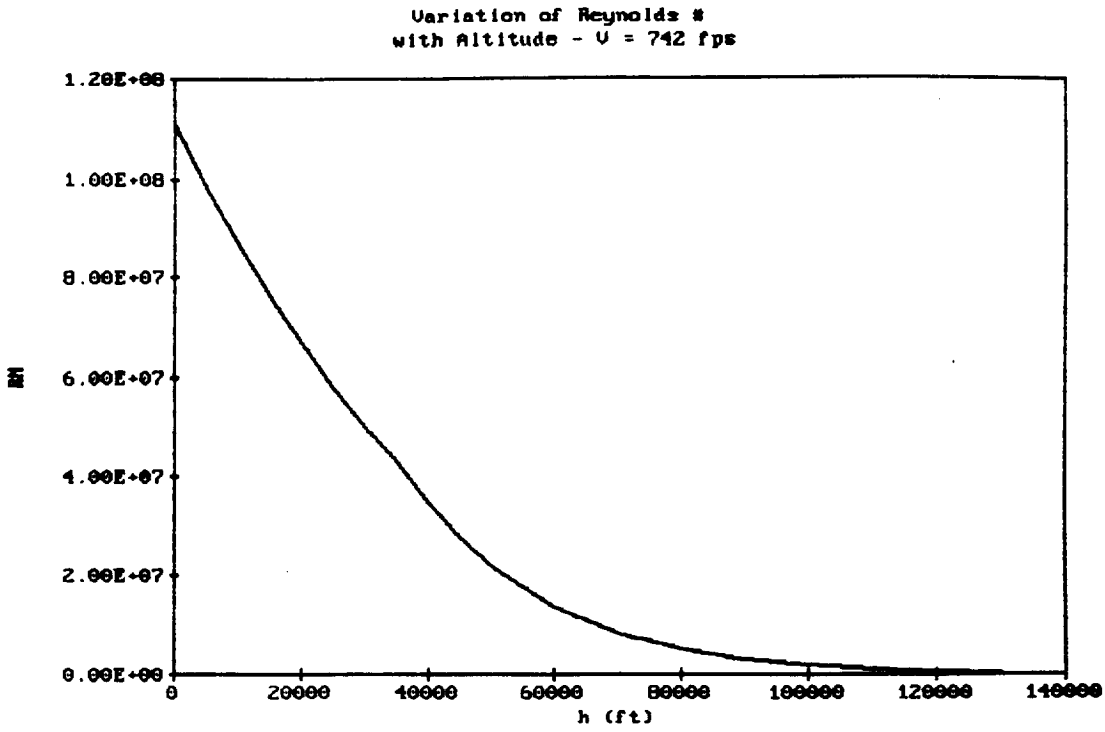

FIGURE 7.6

8.0 **STRUCTURES**

The aircraft was assumed to be composed of three types of structural elements. The three elements are stiffened shells, stiffened plates, and beams. The center fuselage as well as the twin booms are stiffened shells. The top and bottom of main wing stiffened plates. The wing itself is supported by beams extending from the fuselage and ending at the wing tips.

8.1 STRUCTURAL ANALYSIS

A static load analysis was performed to determine the structural integrity of the main wing for the preliminary design. Two flight conditions were simulated in this analysis; normal flight, n = 1 g, and flight experiencing the maximum gust load factor, n = 6.8 g.

8.2 FINITE ELEMENT ANALYSIS

The wing planform was modeled for the half-wing section. The structural arrangement of the wing consisted of spars, ribs, and skin stiffeners. Spar members are continuous along the wing span and form a torque-box (wing box) carrying the main load component. The ribs are segmented elements that help stabilize the skin elements.

The wing structure was modeled on computer using the MSC/NASTRAN software package. A finite element analysis of the model was performed to optimize the distribution of stress on the internal structure of the wing. The wing skin material used in the analysis was graphite epoxy with the following properties; E1=30x106psi, E2=0.75x106psi, v12=0.25, and G12=0.375x106psi. The stacking sequences for the angle-ply symmetrical laminates were 0, 45, and 90 degrees. The thickness of the wing skin was 0.5 inches. The wing was discritized into 5 spars and 25 ribs, 9.81 feet apart. The upper and lower surface of each rib has 10 nodes (spar-rib junctions). Thus the entire wing has 260 nodes

and over 780 degrees of freedom since each node has 3 degrees of freedom. This network of spars and ribs is covered with a machined graphite epoxy skin on both the top and bottom surfaces. Graphite expoxy laminate was chosen for the wing model because of its relative high static strength, long fatigue life, and resistance to corrosion. Moreover, graphite epoxy can be fabricated for a lower cost when compared to similar metallic structures. The finite element model of the wing is given in Figure 8.1. The wing was modeled in a local rectangular coordinate system. The local coordinate system for the wing has the X-axis positive outboard, the Y-axis positive toward the leading edge, and the Z-axis positive up based on the right-hand rule.

8.3 CONSTRAINTS

The constraints on the model were created to counter any unbalanced rotation on a wing. Since spanwise elliptical lift distribution was the main loading on the HI-BI wing model, only minimal amounts of constraints were applied. The constraint points were put along ribs were the wing model was attached to the fuselage. All three translational and rotational degrees of freedom were constrained at these wing root nodal points. The nodal points along the rest of the wing were free to translate and rotate in the X< Y, and Z direction.

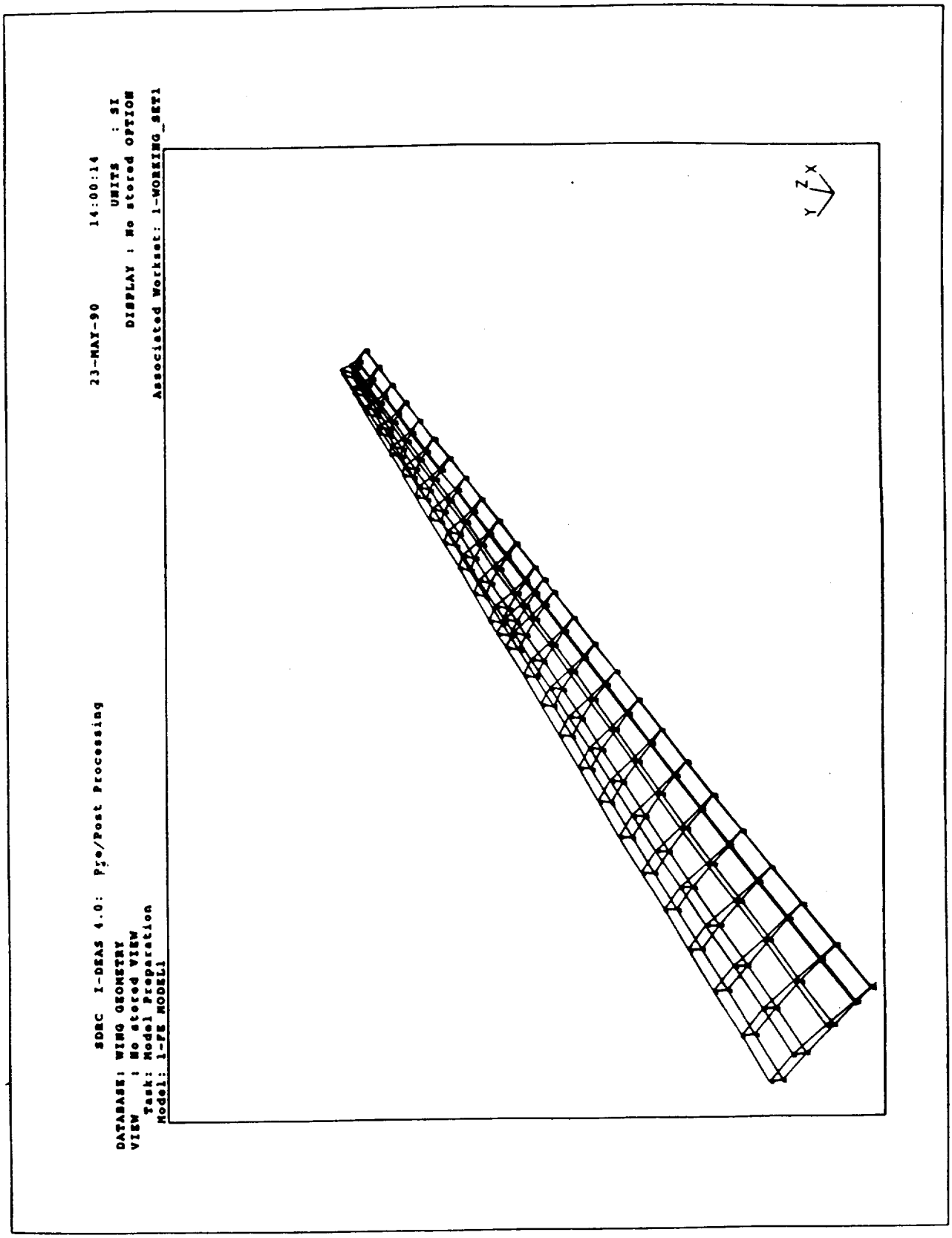

Figure 8.1

8.4 LOADING OF THE MODEL

A V-n maneuver and V-n gust diagram was constructed for the aircraft for two flight conditions, Figures 8.2 thru 8.3. The flight conditions considered were; steady level flight at sea level and steady level flight at the cruise altitude. The positive load factors at cruise are 3.5 and -1.2. The critical load factors were shown to occur at sea level where they 6.8 and -3.7.

Once the critical load factors were determined, the wing spanwise elliptical lift distribution of the appropriate load can be obtained by the following:

$$L' = L'_o \, (1 - (y/(b/2/))^2)_{1/2}$$

where, y...Spanwise location along the x axis measured from the centerline of the wing.

L'_o...Lift per unit span at the center of the wing.

b...Wing span

The results of the applied loads analysis are tabulated in Table 8.1. The wing spanwise elliptical lift distribution accounts only for aerodynamic loading. The total load on the wing structure is composed of the aerodynamic load, the structural weight load, the fuel weight load, and the engine weight load. The aerodynamic loads are much greater than the weight loads and act in a direction opposite the weight loads. The net effect of including the weight loads in the analysis is that the overall structural load is reduced.

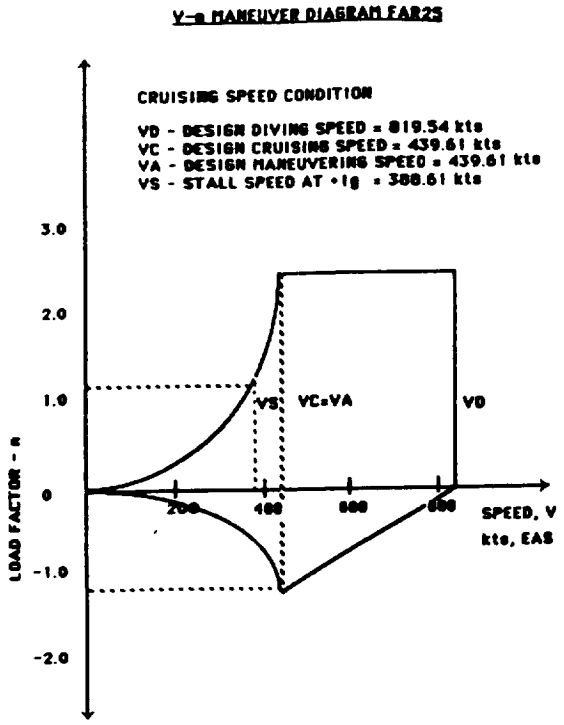

Figure 8.2

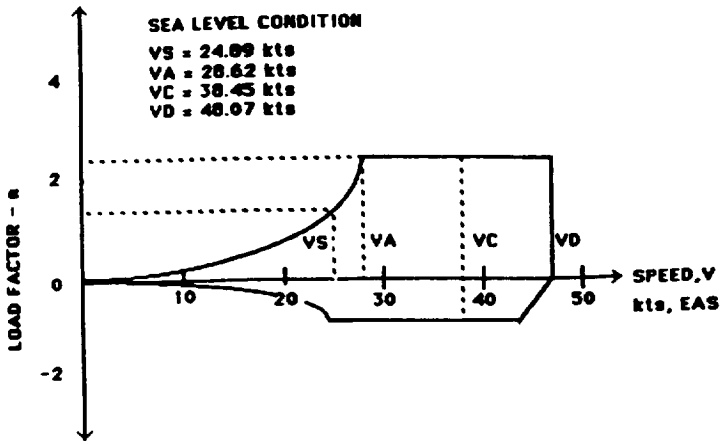

Figure 8.3

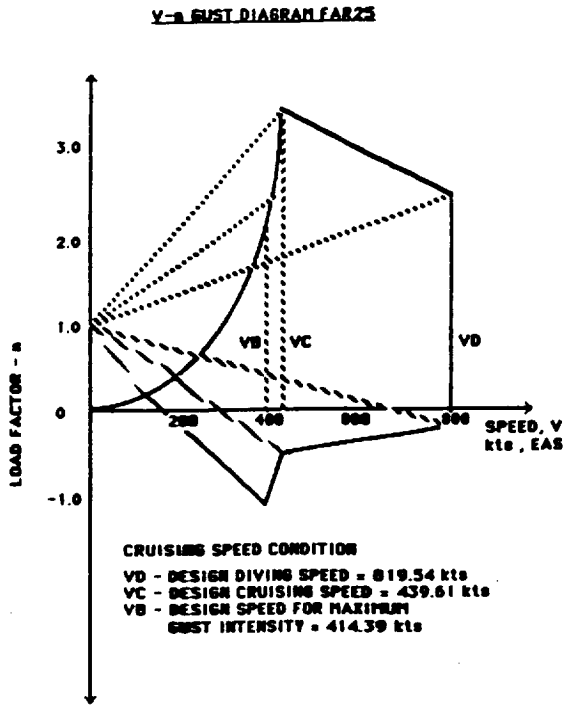

Figure 8.4

TABLE I: WING LOAD DISTRIBUTION (n = 1g)

SPAN b/2	LIFT/ SPAN (lb/ft)	PLOAD1 1st Spar (lb/ft)	PLOAD1 2nd Spar (lb/ft)	PLOAD1 3rd Spar (lb/ft)	PLOAD1 4th Spar (lb/ft)	PLOAD1 5th Spar (lb/ft)	WING WEIGHT (lb/ft)	FUEL WEIGHT
0.00	169.89	35.31	45.94	37.68	29.75	21.21	-21.41	-31.86
9.81	169.75	35.28	45.90	37.64	29.73	21.19	-19.66	-29.26
19.62	169.30	35.18	45.78	37.55	29.65	21.14	-17.99	-26.77
29.43	168.56	35.03	45.58	37.38	29.52	21.05	-16.39	-24.39
39.24	167.52	34.81	45.30	37.15	29.34	20.92	-14.87	-22.12
49.05	166.17	34.53	44.93	36.85	29.10	20.75	-13.42	-19.96
58.86	164.50	34.19	44.48	36.48	28.81	20.54	-12.04	-17.92
68.67	162.51	33.77	43.95	36.04	28.46	20.29	-10.74	-15.98
78.48	160.18	33.29	43.32	35.52	28.05	20.00	-9.51	-14.16
88.29	157.50	32.73	42.59	34.93	27.58	19.67	-8.36	-12.44
98.10	154.44	32.10	41.76	34.25	27.05	19.28	-7.28	-10.84
107.91	151.00	31.38	40.83	33.49	26.44	18.85	-6.28	-9.35
117.72	147.13	30.58	39.79	32.63	25.77	18.37	-5.35	-7.96
127.53	142.81	29.68	38.62	31.67	25.01	17.83	-4.50	-6.69
137.34	137.99	28.68	37.32	30.60	24.17	17.23	-3.72	-5.53
147.15	132.62	27.56	35.86	29.41	23.23	16.56	-3.01	-4.48
156.96	126.63	26.32	34.24	28.08	22.18	15.81	-2.38	-3.54
166.77	119.92	24.92	32.43	26.60	21.00	14.97	-1.82	-2.71
176.58	112.37	23.35	30.39	24.92	19.68	14.03	-1.34	-1.99
186.39	103.80	21.57	28.07	23.02	18.18	12.96	-0.93	-1.38
196.20	93.91	19.52	25.40	20.83	16.45	11.73	-0.59	-0.88
206.01	82.25	17.09	22.24	18.24	14.40	10.27	-0.33	-0.50
215.82	67.90	14.11	18.36	15.06	11.89	8.48	-0.15	-0.22
225.63	48.53	10.09	13.12	10.76	8.50	6.06	-0.04	-0.06
235.44	0.00	0.00	0.00	0.00	0.00	0.00	0.00	0.00

8.5 DEFLECTION

Figure 8.5 and 8.6 show the wing deflection in the x, y and z directions. The deflections in the x and y direction under a 1.0 g load were 3.42 x 10^-2 feet and -2.9 x 10^-2 feet, respectively. The displacement in the positive z direction was determined to be 2.84 feet. At the critical load factor of 6.8 g, the maximum deflections in the x and y directions were -2.16 x 10^-1 feet and -1.75 x 10^-1 feet, respectively. The maximum deflection in the z direction was 15.7 feet.

8.6 TSAI-HILL FAILURE CRITERIA

The Tsai-Hill theory was used to determine if the graphite epoxy would fail in the NASTRAN finite element program. The Tsai-Hill equation yielded a failure index between zero and 0.894. The failure indices were below one which indicates that the graphite epoxy will not fail.

8.7 STRESS

The minor and major principal stresses under the normal flight condition of 1 g, were found to be -1.59 ksi and 1.26 ksi, respective. The limit load factor of 6.8 g applied to the aircraft yielded minor and major stresses of -10.83 ksi and 7.43 ksi, respectively.

DEFLECTION DUE TO LIFT

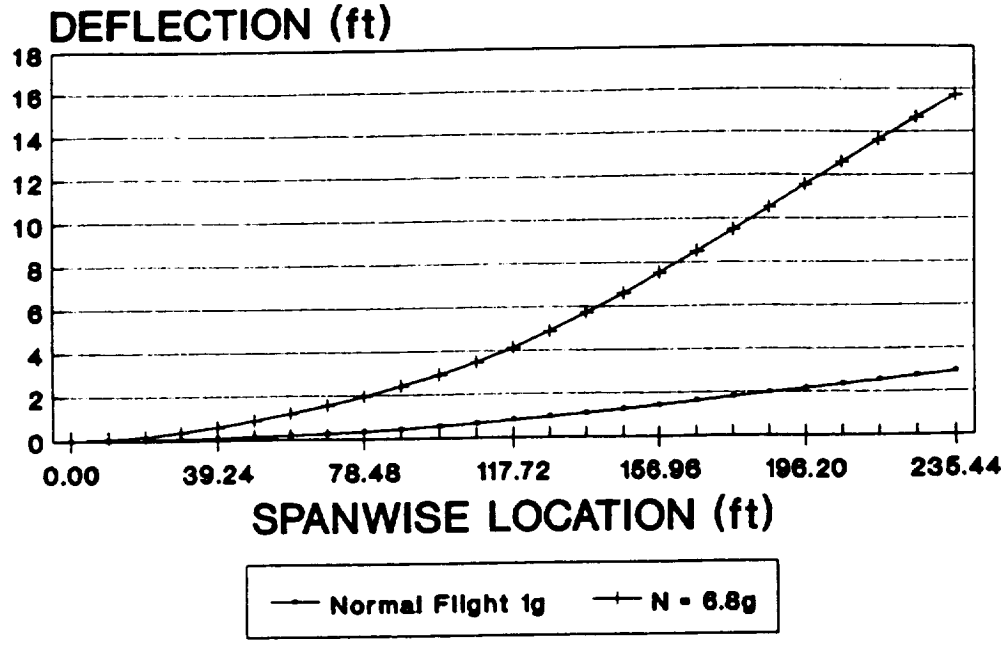

Figure 8.5

DEFLECTION DUE TO DRAG

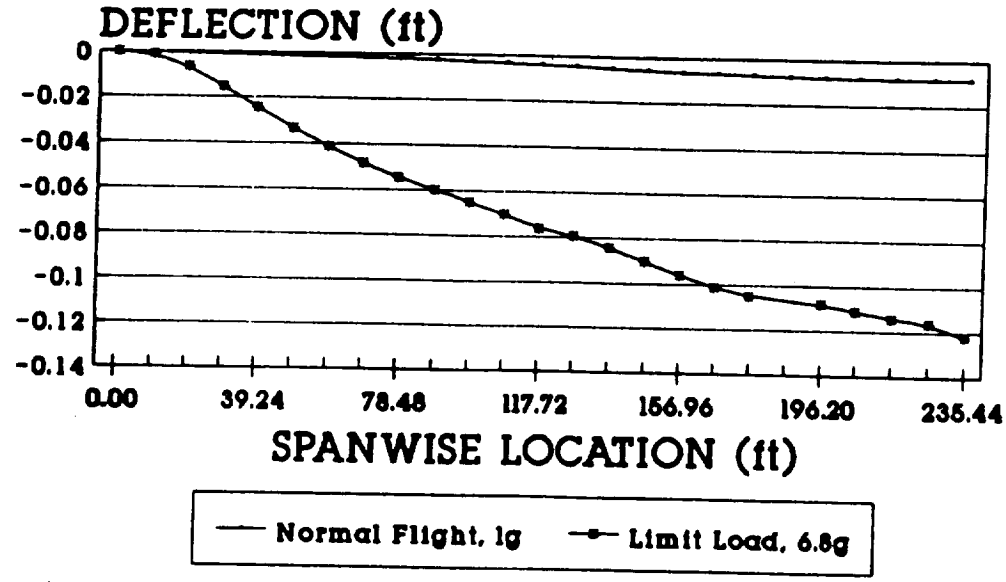

Maximum Wing Deflection:
n = 1g, Y = -.008 ft
n = 6.8g, Y = -.122 ft

Figure 8.6

8.8 BENDING MOMENT

The finite element analysis showed that for the normal flight condition of 1 g, the maximum bending moment occurred at the 4th spar. The bending moments for this point are listed below:

Normal Flight (n = 1g)

$$Mz = 1.42 \times 10^4 \text{ ft-lb}$$

$$My = -1.04 \times 10^4 \text{ ft-lb}$$

The bending moments for the limit load factor of 6.8g were determined for the wing. The results are listed below:

Limit Load Factor (n = 6.8 g)

$$Mz = 1.2 \times 10^5 \text{ ft-lb}$$

$$My = 5.08 \times 10^4 \text{ ft-lb}$$

9.0 LANDING GEAR

9.1 LANDING GEAR ARRANGEMENT

The HI-BI's gear is a tricycle configuration and is shown in Figure 9.1. The nose gear is 25.3 feet in front of the center of gravity (c.g.) with a forward swept angle of 41 degrees. Also, the nose gear structure is tilted 7.5 degrees backward. On the other hand, the main gear is 5.9 feet behind the c.g. with an aft swept angle of 15.0 degrees. Looking at a bottom view of the HI-BI (Figure 9.2), the main gear is 34.1 feet from the aircrafts

LANDING GEAR PLACEMENT W.R.T. CENTER OF GRAVITY

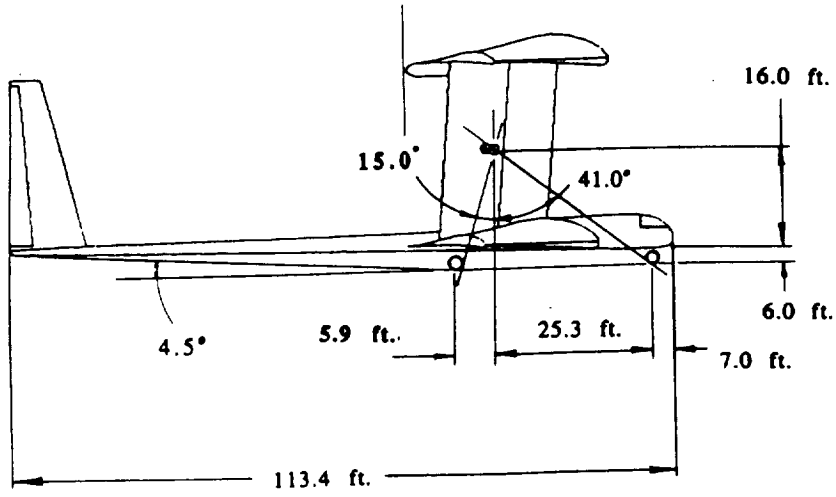

Figure 9.1

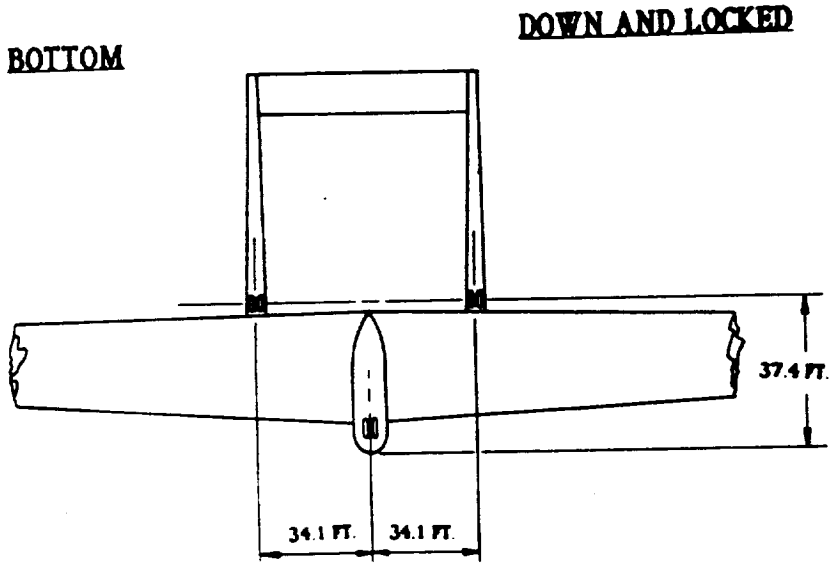

Figure 9.2

centerline, and is 37.4 feet from the nose. The landing gear employs a floating link system with the main retracting forward into the wings and the nose retracting rearward into the fuselage.

9.2 RUNWAY LOADS

Static load analysis was performed on the gears to determine the normal forces acting on the runway (per Reference 11). Alowing for a 25% airplane growth, the following loads resulted:

1) A main gear static load equal to 10864.7 lbs.
2) A nose gear static load equal to 5401.8 lbs.
3) A nose gear dynamic load equal to 12569.8 lbs.

9.3 LANDING GEAR TIRES

The tire selections were based on compatability with large well maintained runways. Table 9.1 shows the tires chosen for the HI-BI.

9.4 SHOCK ABSORBERS

Each gear has a single oleo-pneumatic strut with an axle fastened directly to the strut piston. The main gear shock absorbers are 30.4 inches long by 6 inches in diameter and each are capable of absorbing 560,532.5 ft-lbs of kinetic energy. Conversely, the nose gear shock absorber measures 39.0 inches by 6.2 inches and withstands 568,490.0 ft-lbs of knietic energy.

SELECTED TIRES

MAIN:
* TYPE VII
* TIRE O.D. = 24 IN.
* MAX. WIDTH = 7.7 IN.
* UNLOADED INFLATION PRESSURE = 180 PSI.
* MAX. LOADING = 11,900 LBS.
* WEIGHT PER TIRE = 36.0 LBS

NOSE:
* TYPE VII
* TIRE O.D. = 22 IN.
* MAX. WIDTH = 6.6 IN.
* MAX. LOADING = 5,700 LBS.
* UNLOADED INFLATION PRESSURE = 190 PSI.
* WEIGHT PER TIRE = 21.0 LBS

Table 9.1

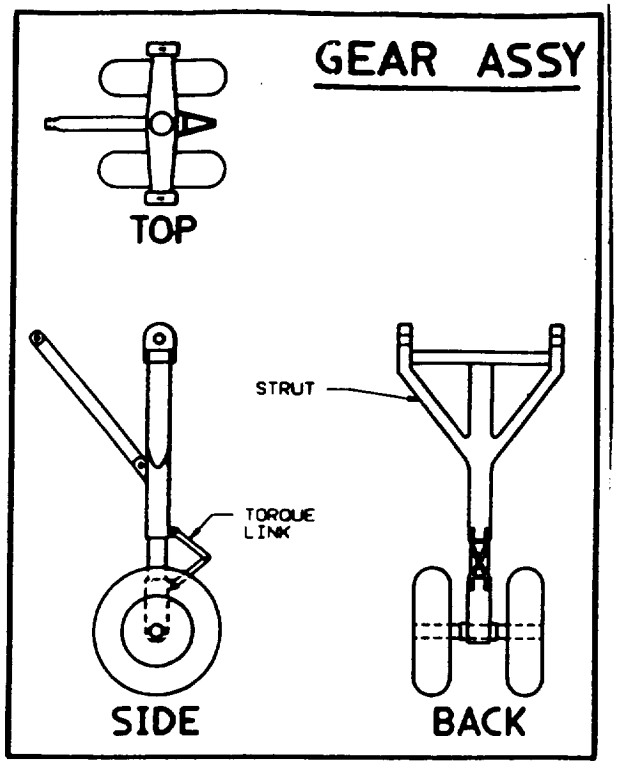

Figure 9.3

9.5 GEAR STRUCTURE

The gear structure was scaled from an aircraft with approximately the same take off weight. The geometry is shown in Figure 9.3. It's made of steel alloy and weighs about 1600 lbs. The main gears are fastened to spars located in the booms, and the nose gear is fastened to the spars in the fuselage.

9.6 LANDING GEAR HYDRAULIC SYSTEM

The HI-BI utilizes a state-of-the-art light weight 8000 psi primary system with titanium lines. The working fluid is Chlorotrifluoroethylene (CTFE), a nonflammable fluid. It's fastened to the HI-BI's fuselage. An emergency pneudraulic back up system is also located in the fuselage. The redundant system generates 3000 psi manually.

9.7 BRAKE SYSTEM

Each main gear has an independent braking system. The system uses CTFE at 8000 psi through its titanium fluid lines. Anti-skid carbon brakes are installed in each main wheel. It features a five rotor brake with an oversized insulating ring. Each brake is self-bleeding and contains a temperature sensor. The pilot controlls each brake seperately. To illustrate, the pilot depresses the right rudder toe pedal to actuate the right-hand wheel, and depresses the left toe rudder to actuate the left-hand wheel.

10.0 RELIABILITY AND MAINTAINABILITY

The reliability of the aircraft was determined using statistical data compiled at the Northrop corporation. The data that was looked at was the MTBF (mean time between failure) and MTBM (mean time between maintenance). Based on these data, the operating hours, sorties, MTBM and MTBF of the 11 major systems, the corresponding systems on the HI-BI aircraft were given a complexity or simplicity factor based on the particular design and component. It was determined that 82% of all failures are inherent and 18% are induced. Further 45% of all maintenance is inherent, 10% induced and 45% are no defects maintenance.

Eleven main systems were looked at in the reliability analysis; namely the airframe, fuselage, landing gear, flight control, electric power supply, lighting system, fuel system, instrumentation, radio and engines. Then average mission duration for the HI-BI was calculated to be 13 hours. Each component was given a reliability percentage based on the compiled data for each component. The initial statistical analysis considered strictly a non-redundant series configuration. This configuration assumes that if any individual component of the aircraft fails, then the whole aircraft would be unoperational. Using this concept, the reliability of the aircraft after 14 hours of flight came out to be approximately 68%, which is not a good

overall reliability. Thus, the non-redundant approach proved to be overly conservative and unrealististic.

A more realistic approach was then taken in the statistical analysis. This approach considers only the major systems; namely the airframe, fuselage, engines, fuel system, and flight controls. This approach yielded a reliability percentage of 78 % for the 13 hour mission, shown in Figure 10.1.

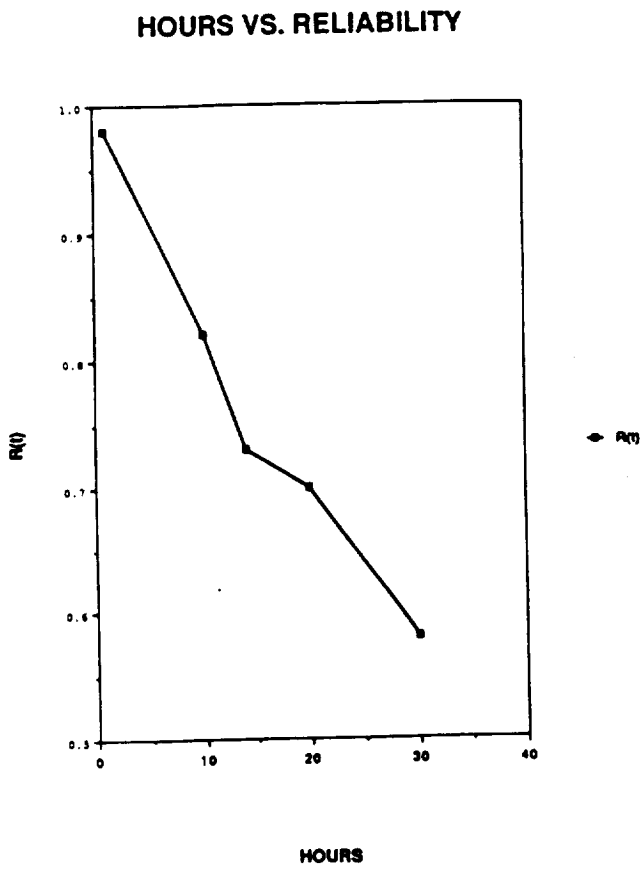

FIGURE 10.1

The maintainability is also a major part of the project. In Figure 10.2, the eleven systems have been illustrated along with their maintainability constants. This constant explains the number of times the system needs maintenance before failure, therefore the lower the maintainability constant the better off the system is. As it one can see in figure 10.2, the main areas of concern would be the engines, the fuselage and the airframe.

In order to calculate the mission availability and equipment availability, a maintainability and availability analysis program was used to calculate these variables for each hour of operation of each system. The program and output can be reviewed in appendix C.

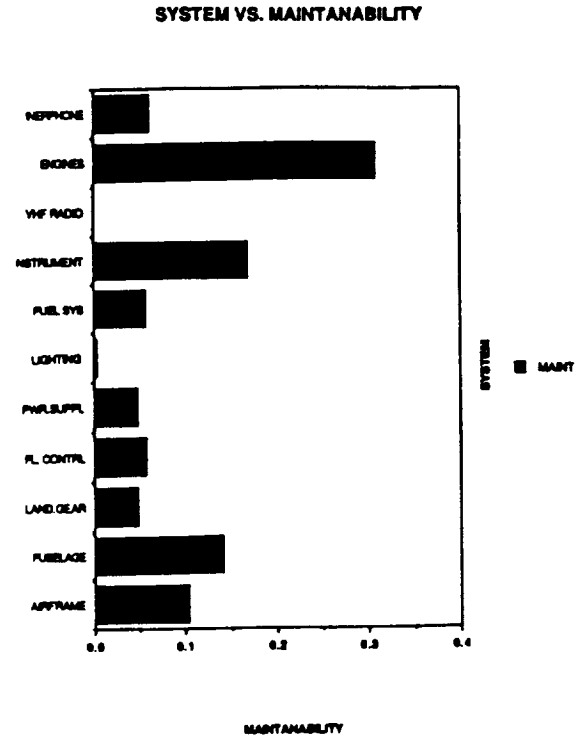

FIGURE 10.2

11.0 COCKPIT VISION AND HUMAN FACTOR

The cockpit was designed to provide the pilot with the standard field of vision 15 degrees below the line of sight as shown in Figure 11.1. The cockpit also had to accommodate the standard pilot. A study was performed to determine the average size of a male pilot. Body component weights are for a male pilot with a weight of 179.3 lbs. are as following:

BODY COMPONENT	WEIGHT IN LBS
Head and neck	15
Upper torso	49
Lower torso	28
Upper legs	39.9
Lower legs and feet	29.8
Upper arms	9.9
Lower arms and hands	7.7
	179.3

The figures for the dimensions and weights would have to be 85% of male pilot for a female pilot. It was decided that we can not deviate from this particular weight and dimension due to the nature of the aircraft design.

The figure 11.2 illustrates how the exact geometry and configurations of the human body and how it is implemented in the cockpit design of figure 11.1.

PILOT LINE OF SIGHT

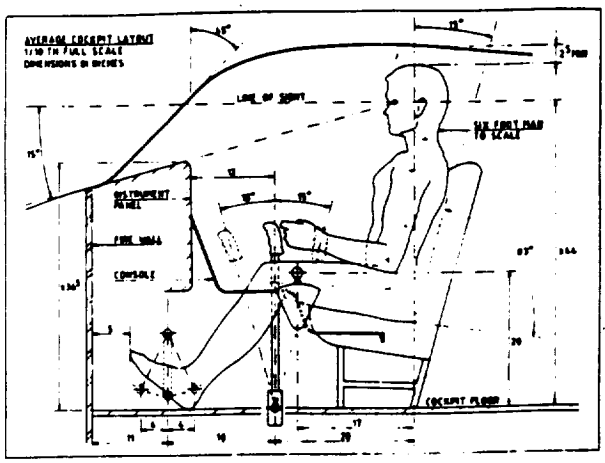

FIGURE 11.1

HUMAN GEOMETRY

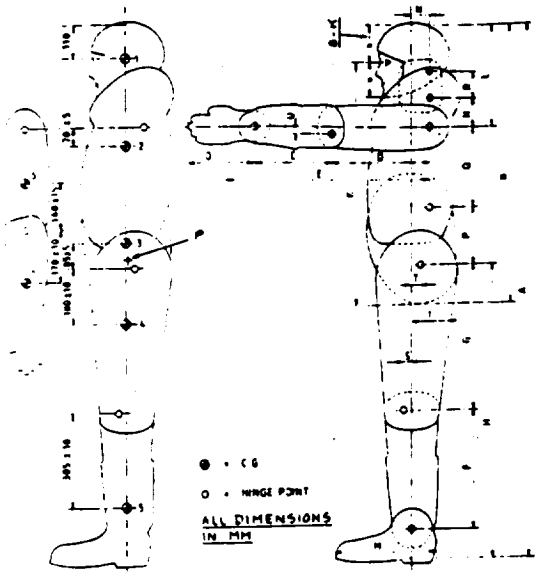

FIGURE 11.2

12.0 COST ANALYSIS

In order to come up with an estimate of the cost, historical data had to be looked into to utilize the regression methods of forecasting more efficiently. The cost of manufacturing, tooling and engineering were looked at. Also relationships were examined that would explain values of time put into different aspects of the aircraft. The variables that proved to have the greatest explanatory values were AMPR weight, maximum speed and the quantity. Exponential regression models have been used to fit the best statistical curves. Incidentally, these equations provide coefficient of correlation from 83% to 97% which is good for estimating cost. In fact, most contractors use the same ideology to estimate the expenses. Some of the breakdowns are as following:

1. Engineering: By using these exponential equations, engineering hours could be estimated, which could then be used to determine engineering cost.
2. Development support: This cost encompasses the cost of manufacturing labor and material required to produce mock-ups, test parts, static test items and other items of hardware.
3. Flight test operations: This category includes performance reliability, stability, control characteristics and air worthiness etc. this also includes engineering planning and data reduction, manufacturing support, instrumentation,

spares, fuel, oil and pilots' pay, facilities rental.

4. Tooling: Tooling hours are defined as hours charged for tool design, tool planning, tool fabrication, production test equipment, check out of tools, maintenance of tooling, normal changes and production planning.

5. Manufacturing labor hours: This includes labor hours necessary to machine, process, fabricate and assemble the major structure and to install purchased parts, administration and off site manufacturing assemblies. Based on this, the cost will be forecasted.

6. Manufacturing materials: This includes the raw material, hardware and purchase of parts required for the fabrication and assembly of the major structure of an aircraft.

7. Quality control: quality control is closely related to direct manufacturing labor, but is estimate separately, since records of actual hours for quality control are not normally included in general manufacturing hours data. On the average, it amounts to approximately 13% of the total labor hour.

The following are the project constraints:

1. The AMPR weight:	25000 lbs.
2. The speed of aircraft:	400 kn
3. The prototype quantity:	1
4. The production quantity:	4
5. The due date of production:	1998
6. The value of learning curve:	.8

The learning curve of 0.8 is standard in the aerospace industry and based on the 0.8 learning curve it was decided to produce 4 aircraft. Also due to inflation and the nature of the equations used, a program was written to convert the dollar values to the value of 1998. So all the dollars values are based on the final completion of the project. In order to come up with a flexible way of computing the values, a program was written and is shown in appendix B.

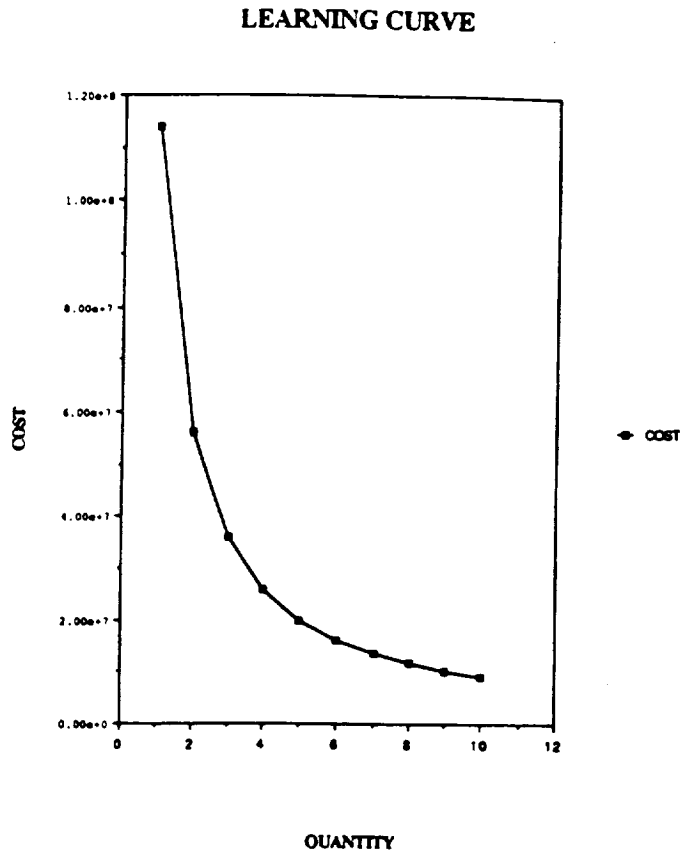

FIGURE 12.1

The following is the breakdown of the cost. The final cost per aircraft was determined using the standard 0.8 learning curve.

Production development cost:	$34,015,730
Production quality control cost:	$12,960,270
Production manufacturing labor cost:	$54,632,060
Production test flight operation cost:	$15,162,880
Production engineering cost:	$42,920,540
Production tooling cost:	$45,223,450
Production total cost:	$349,832,800
Production cost per aircraft:	$78,481,090
Learning curve value per aircraft:	$25,889,100

13.0 MANUFACTURABILITY

The decision was made to manufacture four production aircraft and one prototype. The production of these aircraft during the span of 8 years requires certain number of employees in tooling, engineering and manufacturing. Assuming 50% allocated to R&D and 50% allocated to production and assuming 2000 working hours allocated to each employee. The following figures were obtained.

Total number of employees in engineering:	179
Total number of employees in tooling:	270
Total number of employees in manufacturing:	350

	799

14.0 ELECTRICAL SYSTEM

The HI-BI has four independent electrical systems. The electrical power - under normal operating conditions - is aquired by engine driven generators. When reversed, these direct current (DC) generators double as starter motors. The primary power is inverted to alternating current (AC) via DC buses.

Each system is carefully shielded from the effects of lightning. And the crucial buses and wiring bundles are widely seperated. Additionally, all the batteries are shieled from the primary structure and flammable materials.

15.0 LIFE SUPPORT

The pilot will be required to be in a space suit becuase of the low pressure at altitude. Enough oxygen will be carried to complete the 14 hour mission. Even though the pilot will be in a heated space suit, the cabin will be required to be heated to heat the flight instrumentaion.

16.0 CONCLUSION

Although the intent of the design group was to design an aircraft that would be capable of achieving the performance outlined in the RFP, several problems have presented themselves which indicate that the mission cannot be performed with current technology. The problem areas are listed below:

Aerodynamics

The horizontal tail may be too small to generate enough downforce to rotate the aircraft at takeoff. The airfoil was selected for its performance at the cruise Reynolds number rather than its performance at the cruise Mach number. The airfoil might not be able to provide the lift that the aircraft requires.

Propulsion

Supercharging system has yet to be installed on an engine of this size. The actual operating efficiencies may be much lower than estimated because the calculations were single stage units rather than series arrangements. A propeller has yet to be developed that is large enough to produce the thrust required. The problem of cooling the engine has to be solved as the traditional method of convection would not be feasible due to the low dynamic pressures found at cruise.

Structures

The limit load factor did not include a factor of safety. The aircraft would probably be required to withstand higher load factors because it would be manned. Further the structural analysis performed on the aircraft considered only the main wings and the supports. The overall structure will probably need to be redesigned to withstand the high load factors experienced by the aircraft.

Human Factors

The long flight duration of 14 hours is probably too demanding on a pilot. The ER-2 has a similar working environment and pilot workload to the HI-BI. Pilots have much difficulty in withstanding flights longer than 8 hours in the ER-2.

17.0 RECOMMENDATIONS

The 130,000 ft. cruise requirement was the most demanding performance requirement. The cruise altitude should be lowered to an altitude closer to 100,000 feet. At this altitude the dynamic pressure is four times greater for the design Mach number of 0.7.

The 6 hour cruise time also seemed unrealistic. This required the aircraft to carry a large amount of fuel given the difficulty in producing thrust at altitude. Scientist indicate that the long cruise time is required to sample a large section of the ozone layer. An alternative to the long cruise time might be to fly the aircraft at an even lower altitude and climbing to the desired altitude for very brief periods thus sampling a large section of the ozone layer.

REFERENCES

1. Abbott, I. H. and Doenhoff, A. E. Von, "THEORY OF WING SECTIONS", Dover Publications, Inc., 1959

2. Houghton, E. L. and Carruthers, N. B., "Aerodynamics for Engineering Students," Edward Arnold Ltd., 1982

3. Liebeck, R.H. and Camacho, P.P.; "Airfoil Design at Low Reynolds number with Constrained pitching moment"; Douglas Aircraft Company; Long Beach, Ca

4. McCormick, B. W., "Aerodynamics, Aeronautics, and Flight Mechanics," John Wiley and Sons, 1979

5. MIL-F-8785B (ASG) Military Specification - Flying Qualities of Piloted Airplanes, August 1969

6. Nicolai, L.M.; "Fundamentals of AIRCRAFT DESIGN"; Aerospace Engineering University of Dayton; Dayton, Ohio, 1984

7. Olson, C.E. and Selberg, B.P.; "Experimental Determination of Improved Aerodynamic Characteristics Utilizing Biplane Wing Configuration"; AIAA paper, University of Missouri- Rolla, Rolla, Missouri, 1974

8. O'Neil, J.D.; "Maintainability and Availability Program", California State Polytechnic University Pomona, Pomona, Ca.

9. Roskam, Jan; "AIRPLANE FLIGHT DYNAMICS AND AUTOMATIC FLIGHT CONTROLS"; University of Kansas; Lawrence, Kansas, 1982

10. Roskam, Jan; "Methods For Estimating Stability And Control Derivatives Of Conventional Subsonic Airplanes"; University of Kansas; Lawrence, Kansas, 1982

11. Roskam, Jan; "AIRPLANE DESIGN PART 4", University of Kansas; Lawrence, Kansas, 1982

12. Shevell, R. S., "Fundamentals of Flight," Prentice-Hall,Inc., 1983

13. Vail, J.T., "Design for Maintainability", SAE Technical Paper

14. AFDA, VERSION 3.2, Aladaire International Inc., 1989

15. Akkerman, J.W., Hydrazine Monopropellant Reciprocating Engine Development. NASA Lyndon B. Johnson Space Center. Houston, Texas, January 1976.

16. Lockheed-California Co., "Stress Concenteration Factors Reference

17. Logan, Daryl L., "A First Course in the Finite Element Method", PWS Publishers, Boston, MA., 1986

18. Schaeffer, Harry G., "MSC/NASTRAN Primer: Static and Normal Modes Analysis", Schaeffer Analysis INC., Mont Vernon, NH

19. Benson, R.S. and Whitehouse, N.D., Internal Combustion Engines. Pergamon Press Inc. New York, 1979.

20. Kays, W.M. and London, A.L., Compact Heat Exchangers, 3rd Edition. McGraw-Hill Book Company. New York, 1984.

21. Zinner, K., Supercharging of Internal Combustion Engines. Springer-Verlag. New York, 1978.

22. Janota, M.S. and Watson, N., Turbocharging the Internal Combustion Engine. John Wiley & Sons Inc. New York, 1982.

23. Campbell, Ashley S., Thermodynamic Analysis of Combustion Engines. John Wiley & Sons Inc. New York, 1979.

24. Benway, Ralph B., Design an Development of a Light Weight, High Pressure Ratio Aircraft Turbocharger. SAE 871041, 1987.

25. High Altitude Atmospheric Research Platform, Information Package. The Lockheed Corporation. Burbank, California. Febuary, 1990.

APPENDIX A

REQUEST FOR PROPOSAL

DESIGN OBJECTIVES AND REQUIREMENTS

REQUEST FOR PROPOSAL: A HIGH ALTITUDE RECONNAISSANCE AIRCRAFT

I. OPPORTUNITY DESCRIPTION

The recent discovery of an ozone hole above the North Pole has prompted the scientific community to accelerate their efforts in investigating man's impact on his environment. The existence of the ozone hole has brought about concern that the predictions of environmentalists may come true. Unless the ozone depletion in the Earth's atmosphere is controlled, radiation levels at the surface may increase to harmful levels. At the equator, the ozone layer ranges from 80,000 to 100,000+ feet which is beyond the capabilities of the ER-2 aircraft, NASA's current high altitude reconnaissance aircraft. Therefore, to effectively investigate the ozone layer, NASA needs to develop a high altitude airlift which will reach altitudes of 100,000+ feet. To hasten the development of the technology and methodology required to develop an aircraft that can reach these altitudes, the NASA program has been working closely with industry and universities. Perhaps, with the data retrieved by this aircraft, scientists and politicians will be able to formulate an emissions control plan which will diminish the rate of degeneration of the ozone layer.

II. PROJECT OBJECTIVE

The objective of this project is to develop three possible designs for an aircraft that can cruise at 100,00+ feet and sample the chemistry of the ozone layer at this altitude. 1 An innovative approach which pushes the limits of existing technology is inherent in the nature of this project. However, the techniques used should be feasible by the year 1990. All operational constraints must be met.

III. REQUIREMENTS AND CONSTRAINTS

1. The cruise altitude will be 130,00 feet.
2. The required payload will be 3,000 pounds.
3. The design cruise Mach number will be M=0.7
4. The cruise (data sampling) time will be six hours
5. There is a minimum of one crew member responsible for piloting the aircraft.
6. A 6,000 mile range is required.

APPENDIX B

COST BREAKDOWN

```
'*************************
'*******COST ANALYSIS*********************************
 THIS PROGRAM WILL FIGURE OUT THE TIME AND COST OF ENGINEERING, TOOLING
 AND MANUFACTURING OF A PROTOTYPE AIR CRAFT AND THE PRODUCTION OF THE
'PARTICULAR AIR CRAFT.
'*********************************MAIN OUT LINE*********************************
CLS
GOSUB INPUTDATA
GOSUB PROTO
GOSUB PROD
GOSUB DEFLATOR
GOSUB COST
GOSUB PRNT
END
'*********************************INPUTDATA*************************************
INPUTDATA:
INPUT "ENTER THE AMPR WEIGHT OF TEH AIR CRAFT"; A
INPUT "ENTER THE SPEED OF AIR CRAFT (KN)"; S
INPUT "ENTER THE PROTOTYPE QUANTITY"; QP
INPUT "ENTER THE PRODUCTION QUANTITY"; Q
INPUT "ENTER NO. YEARS ALLOCATED FOR THE PROJECT"; R
INPUT "THE PERCENT LEARNING"; N
RETURN
'*********************************PROTOTYE**************************************
PROTO:
'ENGINEERING
LET EP = (8.634 * A ^ .576) * (S ^ .856) * (QP ^ .96)
LPRINT "THE TOTAL PROTOTYPE ENGINEERING HOURS ARE"; EP; "HOURS"
 'PROTOTYPE DEVELOPMENT SUPPORT
LET DP = (.06474 * A ^ .802) * (S ^ 2.267) * (QP ^ .485)
'PROTOTYPE TOOLING
LET TP = (57.385 * A ^ .466) * (S ^ .633) * (QP ^ .482)
LPRINT "THE TOTAL PROTOTYPE TOOLING HOURS ARE"; TP; "HOURS"
'PROTOTYPE MANUFACTURING
LET LP = (.3019 * A ^ 1.118) * (S ^ .41) * (QP ^ 1.366)
LPRINT "THE TOTAL PROTOTYPE MANUFACTURING HOURS ARE"; LP; "HOURS"
'PROTOTYPE MATERIAL
LET MP = (1.5 * A ^ .585) * (S ^ 1.213) * (QP ^ .622)
'PROTOTYPE QUALITY CONTROL
LET CQCP = .13 * LP
'PROTOTYPE FLIGHT TEST
LET FP = (.001244 * A ^ 1.16) * (S ^ 1.371) * (QP ^ 1.281)
RETURN
'*********************************PRODUCTION************************************
PROD:
'ENGINEERING
LET E = (.0396 * A ^ .791) * (S ^ 1.526) * (Q ^ .183)
LPRINT "THE TOTAL ENGINEERING HOURS ARE"; E; "HOURS"
'DEVELOPMENT SUPPORT
LET D = (.008325 * A ^ .873) * (S ^ 1.89) * (Q ^ .346)
'FLIGHT TEST OPERATION
LET F = (.001244 * A ^ 1.16) * (S ^ 1.371) * (Q ^ 1.281)
'TOOLING
'ET T = (4.0127 * A ^ .764) * (S ^ .899) * (Q ^ .178) * (2 * Q / (12 * R)) ^ .

LPRINT "THE TOTAL TOOLING HOURS ARE"; T; "HOURS"
'MANUFACTURING HOURS
LET L = (28.984 * A ^ .74) * (S   .543) * (Q ^ .524)
LPRINT "THE TOTAL MANUFACTURING HOURS ARE"; L; "HOURS"
'MANUFACTURING COST
LET M = (37.632 * A ^ .689) * (S ^ .624) * (Q ^ .792)
```

```
END IF
RETURN
'*************************************DEFLATOR*****************************************
DEFLATOR:
'AEROSPACE CPI FOR 1970 IS 35.7
 ET YR = 1990 + R
 CALCULATING THE DEFLATOR
LET LI = YR - 1966
LET CP = 10.91363 + (4.593033 * LI)
IF CP THEN
IR = (CP / 35.7) ^ (1 / (20 + R)) - 1
PIR = 100 * IR
END IF
RETURN
'*************************************COST*********************************************
COST:

IF IR THEN
DI = D * (1 + IR) ^ (20 + R)
DPI = DP * (1 + IR) ^ (20 + R)
MPI = MP * (1 + IR) ^ (20 + R)
FI = F * (1 + IR) ^ (20 + R)
FPI = FP * (1 + IR) ^ (20 + R)
END IF

'ENGINEERING,MANUFACTURING,TOOLING HOURLY RATES
LET TI = YR - 1954
IF TI = YR - 1954 THEN
YE = 5.453 + .555 * TI
YM = 5.184 + .3278 * TI
YT = 5.7488 + .3406 * TI
 ND IF
LET EPI = EP * YE
LET TPI = TP * YT
LET EI = E * YE
LET TT = T * YT
LET MI = M * YM
LET LI = L * YM
LET LPI = YM * LP
LET CQCP = .13 * LPI
LET CQC = .13 * MI

LET A = DPI + MPI + EPI + FPI + LPI + CQCP + TPI
LET B = FI + EI + TT + MI + TT + CQC + DI + LI
LET TOT = A + B + XP

LET X = TOT / (QP + Q)
LET XP = .1 * TOT
'LEARNING CURVE
TX = X / Q ^ N
RETURN
'*************************************PRINT********************************************
PRNT:
PRINT "THE AMPR WEIGHT OF AIRCRAFT"; A
PRINT "THE SPEED OF AIRCRAFT (KN)"; S
PRINT "THE NO. OF PROTOTYPES REQUIRED"; QP
 RINT "THE NO. OF PRODUCTION REQUIRED"; Q
 RINT "THE NO. OF YEARS ALLOCATED FOR PROJECT"; R
PRINT "THE INFLATION RATE BASED ON 1970 FOR"; YR; "IS"; "%"; PIR
PRINT "THE DUE DATE FOR THE PROJECT IS"; YR
PRINT "THE PROTOTYPE DEVELOPMENT COST IS"; DPI; "DOLLARS"
PRINT "THE PROTOTYPE MATERIAL COST IS"; MPI; "DOLLARS"
PRINT "THE PROTOTYPE QUALITY CONTROL COST IS"; CQCP; "DOLLARS"
PRINT "THE PROTOTYPE TEST FLIGHT OPERATION COST IS"; FPI; "DOLLARS"
```

APPENDIX C

MAINTAINABILITY & AVAILABILITY ANALYSIS

```
100 COLOR 7, 9, 1: CLS
110 REM: J.D. O'Neil 5/85
120 PRINT "              MAINTAINABILITY & AVAILABILITY ANALYSIS"
130 PRINT
140 PRINT "This program analyzes a number of different maintenance and avai
150 PRINT "parameters for a system. The user is asked to provide a number c
160 PRINT "specifications and the time interval for the analysis."
170 PRINT "The specifications required are:"
180 PRINT "     (1) The mean time of a maintenance action (phi)"
190 PRINT "     (2) The maintenance time constraint (t)"
200 PRINT "     (3) The system failure rate (lambda or r)"
210 PRINT "     (4) The mission start time (usually =0)"
220 PRINT "     (5) The length of time for the analysis"
230 PRINT "     (6) The time increment for data analysis"
240 PRINT "NOTE -- All times should be in hours."
250 PRINT
260 PRINT
270 PRINT "The program provides the following output:"
280 PRINT
290 PRINT "(1) MAINTAINABILITY - defines the probability that the system wi
300 PRINT "restored to operational effectiveness within a given period of t
310 PRINT "(the maintenance time constraint) when the maintenance action i
320 PRINT "formed in accordance with prescribed procedures."
330 PRINT
340 INPUT "<ENTER> to continue", Z$: CLS
350 PRINT "(2) MAINTAINABILITY INCREMENT - defines the proportion of failur
360 PRINT "the mission which will be restored to operational effectiveness
370 PRINT "maintenance time constraint (t), as a result of maintenance acti
380 PRINT
390 PRINT "(3) EQUIPMENT AVAILABILITY - is the probability that a stated pe
400 PRINT "of equipment will be available for use at a given time due to the
410 PRINT "bined effect of the survivors and to units restored to service t
420 PRINT "maintainability in a time equal to or less that the maintenance t
430 PRINT "constraint."
440 PRINT
450 PRINT "(4) MISSION AVAILABILITY - is the probability that a stated perc
460 PRINT "missions of a given time duration will not have any failure in a
470 PRINT "mission which cannot, through maintainability, be restored to se
480 PRINT "in a time less than or equal to the maintenance time constraint."
490 PRINT
500 PRINT "(5) UP-TIME-RATIO (UTR) - the ratio of the time the system is 'u
510 PRINT "operating to the sum of the down and up time. It is composed of a
520 PRINT "state element (mu/(r+mu)) and a transient element in the early op
530 PRINT "period. UTR+DTR=1."
540 PRINT
550 INPUT "<ENTER> to continue", Z$
560 CLS
570 R$ = "#######.######"
590 E = 2.7182818284#
610 INPUT "Mean time of maintenance action (phi)?                ", PH
620 MU = 1 / PH
630 INPUT "What is the maintenance time constraint (t)?          ", TC
640 B = MU * TC
650 INPUT "What is the system failure rate (failures/hour)?      ", R
660 INPUT "What is the starting time of the analysis?            ", TS
670 INPUT "What is the ending time for the analysis?             ", TE
680 INPUT "At what intervals do you want to see the analysis? "; DT
690 CLS
700 PRINT "Mean maintenance action time (hrs)="; PH
710 PRINT "Maintenance actions per hour ="; 1 / PH
    PRINT "Maintenance time constraint (t) ="; TC
720 PRINT "System failure rate =": R
```

```
740 PRINT USING R$; (1 - E ^ (-B));
750 PRINT
760 PRINT "Mission                    Maintenance    Equipment      Mission
770 PRINT " Hours        UTR          Increment     Availability  Availability
780 FOR T = TS TO TE STEP DT
790 RMU = R + MU: IF T = 0 GOTO 810
800 TRM = T * (RMU ^ 2): MRT = R / TRM
810 IF T = 0 THEN UTR = 1 ELSE UTR = (MU / RMU) + MRT - MRT * E ^ (-(RMU *
820 MD = 1 - E ^ (-R * T) - (E ^ -B) * (1 - E ^ (-R * T))
830 LE = 1 - (E ^ (-B)) * (1 - E ^ (-R * T))
840 LM = E ^ ((-R * T) * E ^ (-B))
850 RT = E ^ (-R * T)
860 PRINT USING "#####"; T;
870 PRINT USING R$; UTR;
880 PRINT USING R$; MD;
890 PRINT USING R$; LE;
900 PRINT USING R$; LM;
910 PRINT USING R$; RT
920 NEXT T
1000 END
```

Mean maintenance action time (hrs)= 182.2
Maintenance actions per hour = 5.488474E-03
Maintenance time constraint (t) = 40

1.000000	0.000000	1.000000	1.000000	1.000000
0.995015	0.001969	0.991979	0.991971	0.990010
0.990099	0.003919	0.984039	0.984007	0.980120
0.985252	0.005848	0.976178	0.976107	0.970329
0.980471	0.007759	0.968395	0.968270	0.960636
0.975757	0.009651	0.960690	0.960496	0.951039
0.971107	0.011523	0.953062	0.952785	0.941539
0.966522	0.013377	0.945510	0.945135	0.932133

Mean maintenance action time (hrs)= 132
Maintenance actions per hour = 7.575758E-03
Maintenance time constraint (t) = 20

1.000000	0.000000	1.000000	1.000000	1.000000
0.995249	0.001340	0.991809	0.991801	0.990460
0.990570	0.002662	0.983691	0.983669	0.981022
0.985879	0.003983	0.975652	0.975603	0.971669
0.981456	0.005286	0.967691	0.967604	0.962405
0.977007	0.006576	0.959805	0.959670	0.953229
0.972630	0.007854	0.951994	0.951802	0.944141
0.968324	0.009119	0.944258	0.943998	0.935139

Mean maintenance action time (hrs)= 160.3
Maintenance actions per hour = 6.238303E-03
Maintenance time constraint (t) = 8

1.000000	0.000000	1.000000	1.000000	1.000000
0.994790	0.000500	0.990063	0.990061	0.989555
0.989659	0.001012	0.980231	0.980221	0.979219
0.984606	0.001510	0.970501	0.970478	0.968991
0.979629	0.002002	0.960872	0.960832	0.958870
0.974727	0.002490	0.951344	0.951283	0.948854
0.969899	0.002972	0.941916	0.941828	0.938944
0.965143	0.003450	0.932586	0.932467	0.929136

Mean maintenance action time (hrs)= 135
Maintenance actions per hour = 7.407407E-03
Maintenance time constraint (t) = 8

1.000000	0.000000	1.000000	1.000000	1.000000
0.994369	0.000650	0.989354	0.989351	0.988704
0.988836	0.001293	0.978829	0.978815	0.977536
0.983397	0.001928	0.968422	0.968391	0.966494
0.978053	0.002556	0.958133	0.958079	0.955577
0.972799	0.003177	0.947960	0.947876	0.944783
0.967636	0.003791	0.937902	0.937782	0.934111
0.962561	0.004398	0.927958	0.927795	0.923560

Mean maintenance action time (hrs)= 160
Maintenance actions per hour = .00625
Maintenance time constraint (t) = 8

1.000000	0.000000	1.000000	1.000000	1.000000
0.996235	0.000368	0.992817	0.992816	0.992449
0.992520	0.000734	0.985608	0.985603	0.984954
0.988855	0.001097	0.978613	0.978601	0.977517
0.985238	0.001457	0.971592	0.971571	0.970135
0.981669	0.001814	0.964623	0.964591	0.962809
0.978146	0.002168	0.957707	0.957661	0.955539
0.974671	0.002520	0.950843	0.950780	0.948323

Mean maintenance action time (hrs)= 2390
Maintenance actions per hour = 1.184101E-04
Maintenance time constraint (t) = 8

1.000000	0.000000	1.000000	1.000000	1.000000
0.999900	0.000001	0.999801	0.999801	0.999800
0.999800	0.000001	0.999601	0.999601	0.999600
0.999700	0.000002	0.999402	0.999402	0.999400
0.999601	0.000003	0.999203	0.999203	0.999200
0.999501	0.000003	0.999004	0.999004	0.999000
0.999401	0.000004	0.998805	0.998805	0.998801
0.999302	0.000005	0.998606	0.998606	0.998601

Mean maintenance action time (hrs)= 402.7
Maintenance actions per hour = 2.483238E-03
Maintenance time constraint (t) = 24

1.000000	0.000000	1.000000	1.000000	1.000000
0.997787	0.000256	0.995826	0.995826	0.995570
0.995588	0.000511	0.991671	0.991669	0.991159
0.993402	0.000766	0.987534	0.987529	0.986768
0.991230	0.001018	0.983415	0.983407	0.982397
0.989072	0.001270	0.979315	0.979302	0.978045
0.986927	0.001521	0.975232	0.975214	0.973712
0.984796	0.001771	0.971169	0.971143	0.969398

Mean maintenance action time (hrs)= 259.2
Maintenance actions per hour = 3.858024E-03
Maintenance time constraint (t) = 46

1.000000	0.000000	1.000000	1.000000	1.000000
0.996974	0.001025	0.994963	0.994961	0.993938
0.993976	0.002043	0.989957	0.989947	0.987914
0.991005	0.003056	0.984981	0.984958	0.981925
0.988061	0.004062	0.980035	0.979994	0.975973
0.985144	0.005062	0.975119	0.975050	0.970057
0.982253	0.006056	0.970233	0.970142	0.964177
0.979389	0.007044	0.965377	0.965253	0.958333

Mean maintenance action time (hrs)= 17725.8
Maintenance actions per hour = 5.641494E-05
Maintenance time constraint (t) = 8

1.000000	0.000000	1.000000	1.000000	1.000000
0.999940	0.000000	0.999880	0.999880	0.999880
0.999880	0.000000	0.999760	0.999760	0.999760
0.999820	0.000000	0.999640	0.999640	0.999640
0.999760	0.000000	0.999520	0.999520	0.999520
0.999700	0.000000	0.999400	0.999400	0.999400
0.999640	0.000000	0.999281	0.999281	0.999280
0.999580	0.000000	0.999161	0.999161	0.999160

Mean maintenance action time (hrs)= 216.1
Maintenance actions per hour = 4.627487E-03
Maintenance time constraint (t) = 80

1.000000	0.000000	1.000000	1.000000	1.000000
0.997701	0.001420	0.996017	0.996015	0.995991
0.995422	0.002846	0.992048	0.992039	0.990803
0.993165	0.004259	0.990494	0.990474	0.986236
0.990929	0.005665	0.987355	0.987319	0.981690
0.988712	0.007065	0.984230	0.984174	0.977165
0.986517	0.008459	0.981120	0.981039	0.972661
0.984341	0.009846	0.978023	0.977914	0.968177

Mean maintenance action time (hrs)= 250
Maintenance actions per hour = .004
Maintenance time constraint (t) = 10

1.000000	0.000000	1.000000	1.000000	1.000000
0.996686	0.000412	0.993774	0.993772	0.993362
0.993405	0.000820	0.987589	0.987584	0.986768
0.990155	0.001226	0.981445	0.981433	0.980218
0.986937	0.001630	0.975341	0.975321	0.973712
0.983749	0.002030	0.969279	0.969247	0.967248
0.980593	0.002428	0.963256	0.963211	0.960828
0.977467	0.002824	0.957274	0.957213	0.954450